TÜBİTAK

Turkish Journal of Botany

http://journals.tubitak.gov.tr/botany/

Research Article

Turk J Bot
(2014) 38: 566-594

doi:10.3906/bot-1305-52

SEM analysis of the epibenthic diatoms on *Eudendrium racemosum* (Hydrozoa) from the Mediterranean Sea

Tiziana ROMAGNOLI[1], Cecilia TOTTI[1], Stefano ACCORONI[1], Mario DE STEFANO[2], Chiara PENNESI[1,*]

[1]Department of Life and Environmental Sciences, Faculty of Science, Polytechnic University of the Marche, Ancona, Italy
[2]Department of Environmental, Biological and Pharmaceutical Science, and Technology, 2nd University of Naples, Caserta, Italy

Received: 23.05.2013 • **Accepted:** 25.02.2014 • **Published Online:** 31.03.2014 • **Printed:** 30.04.2014

Abstract: In this work, the valve fine structure, morphology, and dimensions of the epibenthic diatoms living on the marine hydroid *Eudendrium racemosum* Cavolini were investigated through SEM analysis. Hydroid samples were collected from the Ligurian Sea (Mediterranean Sea), from October 2002 to October 2003, with monthly frequency, allowing definition of the annual cycle of diatom communities. Following several taxonomic/systematic papers, this floristics paper documents 32 new records of diatoms (13 araphid, 17 biraphid, 2 monoraphid), which have been classified into different growth forms (adnate, erect, motile, tube-dwelling). Moreover, new information on morphologic data and biodiversity in the Mediterranean Sea are offered, indicating their ecological preferences.

Key words: Biodiversity, epizoic diatoms, *Eudendrium racemosum*, microphytobenthos, morphology, scanning electron microscopy

1. Introduction

Benthic diatoms of shallow coastal marine areas give a reliable contribution to the dynamics of aquatic ecosystems in terms of primary production, nutrient fluxes, and roles in the trophic web (MacIntyre et al., 1996; Totti, 2003). Communities of benthic diatoms can develop associated to different substrata, from the soft bottom (epipelon, epipsammon, and endopelon) (Totti, 2003) to rocks (epilithon) (Totti et al., 2007; Çolak Sabancı and Koray, 2010), macroalgae and seagrasses (epiphyton) (Totti et al., 2009; Pennesi et al., 2011, 2012, 2013; Çolak Sabancı, 2012; Majewska et al., 2013; Lobban and Pennesi, 2014), and animals (epizoon) (Round, 1971; Romagnoli et al., 2007). The peculiar microenvironments provided by marine animals, i.e. metabolite-rich and potentially grazer-free, are successfully exploited by several pennate diatom genera belonging to araphids, biraphids, and monoraphids (Round, 1981). Pennate diatoms are reported to colonize sponges (Cerrano et al., 2004a, 2004b; Totti et al., 2005), hydrozoans (Di Camillo et al., 2005; Romagnoli et al., 2007; Bavestrello et al., 2008), bryozoans (Wuchter et al., 2003), arthropods (Ikeda, 1977; Hiromi and Takano, 1983; Patil and Anil, 2000), mollusks (Gillan and Cadée, 2000; D'Alelio et al., 2011), and vertebrates (Bennett, 1920; Hart, 1935; Holmes, 1985), sometimes with a high degree of host specificity. The main strategy accounts for the development of well-differentiated growth forms, which allow establishing different modes of contact with the substratum: adnate species (both biraphids and monoraphids) strongly adhering horizontally to the substratum by means of the raphidic valve and having limited motility; erect species (araphids, biraphids, and monoraphids) adhering vertically through mucous pads or stalks/peduncles; and motile diatoms (biraphids) having movement capability enabling them to glide above the substratum (Round, 1971; Round et al., 1981). Moreover, it has been pointed out that some species may exhibit more than one growth form, reflecting different strategies of spatial utilization (Hudon and Bourget, 1981; Round et al., 1981; Hudon and Legendre, 1987; Tuji, 1999, 2000; Chen et al., 2010), which are adopted in terms of the competitive advantage obtained.

Among animals, hydroids represent a very suitable habitat for diatom growth. Round et al. (1961) documented different kinds of diatom assemblages, including erect (*Grammatophora* Ehrenberg, *Licmophora* C.Agardh, *Striatella* C.Agardh, *Synedra* Ehrenberg), adnate (*Cocconeis* Ehrenberg), and motile (*Navicula* Bory de Saint-Vincent) genera lying on the hydroid *Amphisbetia operculata* Linnaeus (basionym: *Sertularia operculata* Linnaeus). Dense assemblages of *Cocconeis pseudonotata* De Stefano & Marino have been reported at the border of the theca of the hydroid *Clytia linearis* Thorneley (Di Camillo et al., 2005). Romagnoli et al. (2007) defined

* Correspondence: c.pennesi@univpm.it

the epizoic communities associated with marine hydroid *Eudendrium racemosum* Cavolini in terms of abundance, biomass, and community structure during its annual cycle in the Ligurian Sea.

The present paper provides new detailed morphological information on diatom taxa associated with the marine hydroid *Eudendrium racemosum* from the Ligurian Sea through scanning electron microscopy (SEM) analysis; moreover, some notes about their ecological behavior are given.

2. Materials and methods

Eudendrium racemosum specimens were collected on a concrete quay of the Santa Margherita Ligure harbor (Ligurian Sea; 44°19′52.36″N, 9°12′58.29″E), near a freshwater drain (personal communication) at 0.5 m of depth from October 2002 to October 2003, with a monthly frequency. Samples were fixed in filtered seawater with 4% neutralized formaldehyde. In the laboratory, hydroid colonies were cut into 3 parts (basal, central, and apical) and then put into a glass tube filled with filtered seawater and treated in a sonic bath (BRANSON 2200) to allow the detachment of diatoms from the hydroid stem. Details of this procedure were reported by Romagnoli et al. (2007). Taxonomical determinations have been based mainly on SEM observations. For this purpose, fixed samples were washed with distilled water and cleaned with sulfuric and nitric acids following the von Stosch method (Hasle and Syvertsen, 1996). One or more drops of cleaned material were then poured on a Nucleopore polycarbonate filter fixed on a stub and left to air dry completely. The stub was then sputter-coated with a thin layer of gold-palladium in a Balzer Union evaporator and analyzed by SEM (Philips EM 515 scanning electron microscope). Samples and slides used in this work are stored at the Herbarium of the Polytechnic University of the Marche (Italy), Department of Life and Environmental Sciences (DISVA).

3. Results

Araphid, biraphid, and monoraphid diatom taxa discussed in this paper have been alphabetically listed within each araphid, biraphid, and monoraphid group, starting from orders. Electron microscopy micrographs of analyzed species are illustrated in Figures 1–14. The taxonomical analysis of *Cocconeis* species found, such as *C. convexa* Giffen, *C. dirupta* var. *flexella* (Janisch & Rabenhorst) Grunow in Van Heurck, *C. distans* Gregory, *C. molesta* var. *crucifera* Grunow in Van Heurck, *C. neothumensis* var. *marina* De Stefano et al., *C. scutellum* var. *parva* Grunow in Van Heurck, *C. scutellum* var. *posidoniae* De Stefano et al., *C. scutellum* Ehrenberg var. *scutellum*, and *C. stauroneiformis* (W.Smith; Rabenhorst) Okuno, have not been reported because they were already fully described in the works De Stefano et al. (2000, 2005, 2008) and other authors (Ehrenberg, 1838; Poulin et al., 1984a; Witkowski et al., 2000).

Terminology of frustule morphology in the following accounts is based on Hustedt (1933), Beihette Symposium (1975), Ross et al. (1979), Holmes et al. (1982), Round et al. (1990), and Honeywill (1998). The classification proposed by Round et al. (1990) for suprageneric taxa has been adopted. In the species identification "AA", "TA", and "TS" are used to indicate the apical and transapical axes and the transapical striae, respectively. The striae density was counted at the center of the valve face and also at the margin laterally opposite the center of the valve when the striae were markedly radiate. In monoraphid species the sternum valve and raphe-sternum valve were identified as SV and RSV, respectively (Romero, 1996a, 1996b).

3.1. Araphid diatoms

Cyclophorales

Cyclophoraceae

Cyclophora A.F.Castracane

Cyclophora tenuis Castracane (1878) (Figures 1a–1h)

Refs: Castracane, 1878; Van Heurck, 1880–1885; Peragallo and Peragallo, 1897; Hustedt, 1933; Navarro, 1982b; Podzorski and Håkansson, 1987.

Meas.: AA: 24–53 μm; TA: 4–5.5 μm; TS in 10 μm: 33–40.

Description: Cells rectangular in valve view (Figures 1a and 1b), plate-shaped with rounded ends in girdle view (Figure 1g). Valves slightly convex to linear with well-pronounced mantle (Figures 1c and 1e), often with slightly capitate and broadly rounded ends (Figure 1e). Sternum is linear and narrow (Figures 1c and 1e). A central depression occurs in one valve, while in the other an elliptic or subcircular structure is present (Figures 1b, 1f, and 1g). Valve surfaces show uniseriate striae consisting of circular areolae occluded by hymens (Figure 1e). The internal valve side is similar to the external one (Figure 1d). Girdle consists of several singular bands bearing a single series of poroids (Figures 1g and 1h).

Notes: *Cyclophora tenuis* is an erect form attached to the substrata with mucilaginous pad secreted from the apical pore field; cells form zigzag chains and are each attached by an opposite apical pore field. It occurred on *Eudendrium racemosum* with low densities, mainly in summer, in the apical and middle part of the colony.

Fragilariales

Fragilariaceae

Ardissonea G.De Notaris in G.De Notaris & F.Baglietto

Ardissonea fulgens (Greville) Grunow in Cleve & Grunow (1880) (Figures 1i–1n)

Bas.: *Exilaria fulgens* Greville (1827)

Refs: Cleve and Grunow, 1880; Hustedt, 1933; Patrick and Reimer, 1966; Lobban et al., 2012

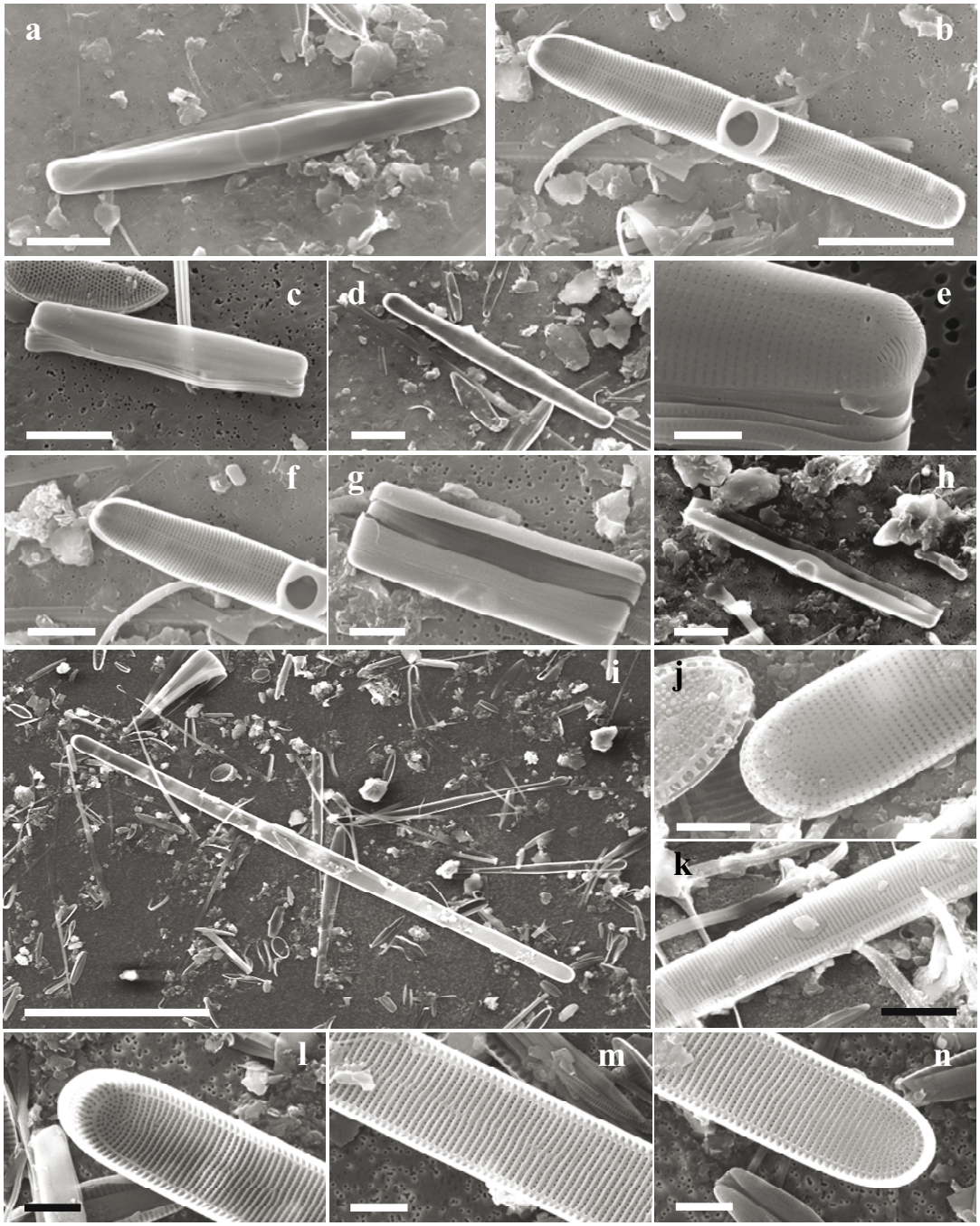

Figure 1. a–h= *Cyclophora tenuis*, SEM. **a=** External valve view showing the imprint of internal subcircular structure in the center. **b=** Internal valve view with a subcircular structure. **c=** External view of the tilted valve. **d=** Internal valve view. **e=** External apex view showing uniseriate striae and the typical elongate curved slits arranged in a distinctive manner. **f=** Internal apex view with uniseriate striae. **g=** Girdle view of the valve showing several bands bearing a single series of circular poroids. **h=** Mantle with expansion close of subcircular structure. **i–n=** *Ardissonea fulgens*, SEM. **i=** Internal valve face. **j=** External polar view with radial striae. **k=** External view of middle valve. **l=** Internal polar view with linear annulus. **m=** Internal central view showing thickened and furcated transapical costae. **n=** Internal view of the apices with uniseriate striae and circular poroids occluded by simple hymens. Scale bars: i = 100 µm; a–d, h, k = 10 µm; f, g, j, l–n = 5 µm; e = 2 µm.

Meas.: AA: 309–370 µm; TA: 11–14 µm; TS in 10 µm: 16–18.

Description: The valve outline is linear and narrow in valve view, slightly swelling in the center (Figure 1i) and at the polar ends (Figure 1j). Valve surfaces slightly convex to linear with pronounced mantle (Figure 1j). Annulus linear and narrow, often not clearly visible in the center of the valve, more evident close to the apices (Figure 1l). Central area absent (Figures 1k and 1m). Valve and mantle striae are uniseriate and consist of circular areolae (Figures 1l–1n). In internal view, transapical costae are sometimes furcated in the valve center (Figures 1l and 1m).

Notes: *Ardissonea fulgens* is an erect form attached to the substrata with a mucilaginous stalk secreted from the apical pore field and forms massive branching colonies. It occurred with low densities on the *Eudendrium racemosum* colony, mainly in winter and spring.

Fragilariales

Fragilariaceae

Diatoma A.P.De Candolle in Lamark & A.P.De Candolle

Diatoma anceps (Ehrenberg) Kirchner (1878) (Figures 2a–2c)

Bas.: *Fragilaria anceps* Ehrenberg (1843).

Refs: Kirchner, 1878; Van Heurck, 1880–1885; De Toni, 1892; Boyer, 1927; Hustedt, 1930; Hustedt, 1933; Patrick and Reimer, 1966; Gasse, 1971.

Meas.: AA: 40–44 µm; TA: 8–9 µm; TS in 10 µm: 25–36; ribs in 10 µm: 10–12.

Description: Cell outline is linear-elliptical with constricted capitate ends in valve view (Figures 2a and 2b). Valve surfaces slightly convex to linear with well-pronounced mantle (Figure 2a). An apical pore field and a rimoportula externally opened by a horizontal slit are visible close to the apices (Figures 2a and 2b). Sternum linear and narrow, missing a hyaline central area. Valve and mantle striae are uniseriate consisting of circular areolae occluded by hymens (Figure 2c). In internal view transapical costae are thickened and irregularly spaced (Figures 2a–2c).

Notes: *Diatoma anceps* is an erect form; cells form straight filamentous colonies, attached on the substrata through a mucus pad. It occurred only occasionally on the *Eudendrium racemosum* colony.

Diatoma vulgare Bory de Saint-Vincent (1831) (Figures 2d and 2e)

Refs: Bory de St-Vincent, 1831; Van Heurck, 1880–1885; De Toni, 1892; Boyer, 1927; Hustedt, 1930; Helmcke and Krieger, 1953; Hustedt, 1933; Begin et al., 1974; Řeháková, 1976; Compère, 1981; Schauderna, 1983; Granetti, 1984; Roemer et al., 1984; Williams, 1985; Luttenton and Rada, 1986; Pickett-Heaps, 1989.

Meas.: AA: 45 µm; TA: 10 µm; TS in 10 µm: 18; ribs in 10 µm: 7.

Description: Cells show a linear-elliptical outline with rounded ends in valve view (Figures 2d and 2e). Valve surface is slightly convex to linear with well-pronounced mantle. Sternum linear and narrow, missing a hyaline central area (Figure 2d). Valve with small circular areolae (Figure 2e). Close to the apices a single rimoportula externally opened by a transapically oriented slit. Apical area of the valve with pore field (Figure 2e).

Notes: *Diatoma vulgare* is an erect form. Cells form zigzag colonies attached to the substrata through a mucus pad. It occurred only occasionally on the *Eudendrium racemosum* colony.

Fragilariales

Fragilariaceae

Tabularia (F.T.Kützing) D.M.Williams & F.E.Round

Tabularia tabulata (C.Agardh) Snoeijs (1992) (Figures 2f–2j)

Bas.: *Diatoma tabulata* C.Agardh (1832).

Refs: Snoeijs, 1992; Hustedt, 1933; Poulin et al., 1986; Round et al., 1990.

Meas.: AA: 13–90 µm; TA: 2–5 µm; TS in 10 µm: 10–29.

Description: Cells linear to lanceolate in valve view (Figures 2f and 2g). Valve face convex, sloping down in a well-pronounced mantle (Figure 2h). Sternum linear to lanceolate missing a central area (Figures 2f and 2h). Externally, transapical striae consisting of single areolae extending from the sternum to the valve margin externally occluded by a cribra with apically oriented bars visible internally (Figures 2i and 2j). An apical pore field with or without a labiate process in each apex (Figures 2h–2j).

Notes: *Tabularia tabulata* is an erect form generally living in little assemblages of single cells directly attached to the substrata by a mucilaginous pad secreted from the apical pore field. It appears as one of the most represented diatom species on *Eudendrium racemosum* colonies. It was observed all year round, with higher density in winter, reaching higher abundances in the upper part of the colony near the polyps.

Licmophorales

Licmophoraceae

Licmophora C.Agardh

Licmophora abbreviata C.Agardh (1831) (Figures 3a–3e)

Refs: Agardh, 1831; Van Heurck, 1880–1885; De Toni, 1892; Peragallo, 1901; Boyer, 1927; Hustedt, 1933; Ohgai et al., 1984; Poulin et al., 1984b; Nikolaev and Dmitrash, 1985; Wahrer et al., 1985; Honeywill, 1988.

Meas.: AA: 43–97 µm; TA: 6–9 µm; TS in 10 µm: 11 near basal pole, 15 near head pole.

Description: Cells heteropolar, clavate in valve view, showing a narrow sternum (Figures 3a and 3b). Valve surface slightly convex with a well-pronounced mantle near the round head pole (Figure 3d) becoming shorter close to the foot pole (Figure 3e). Transapical striae

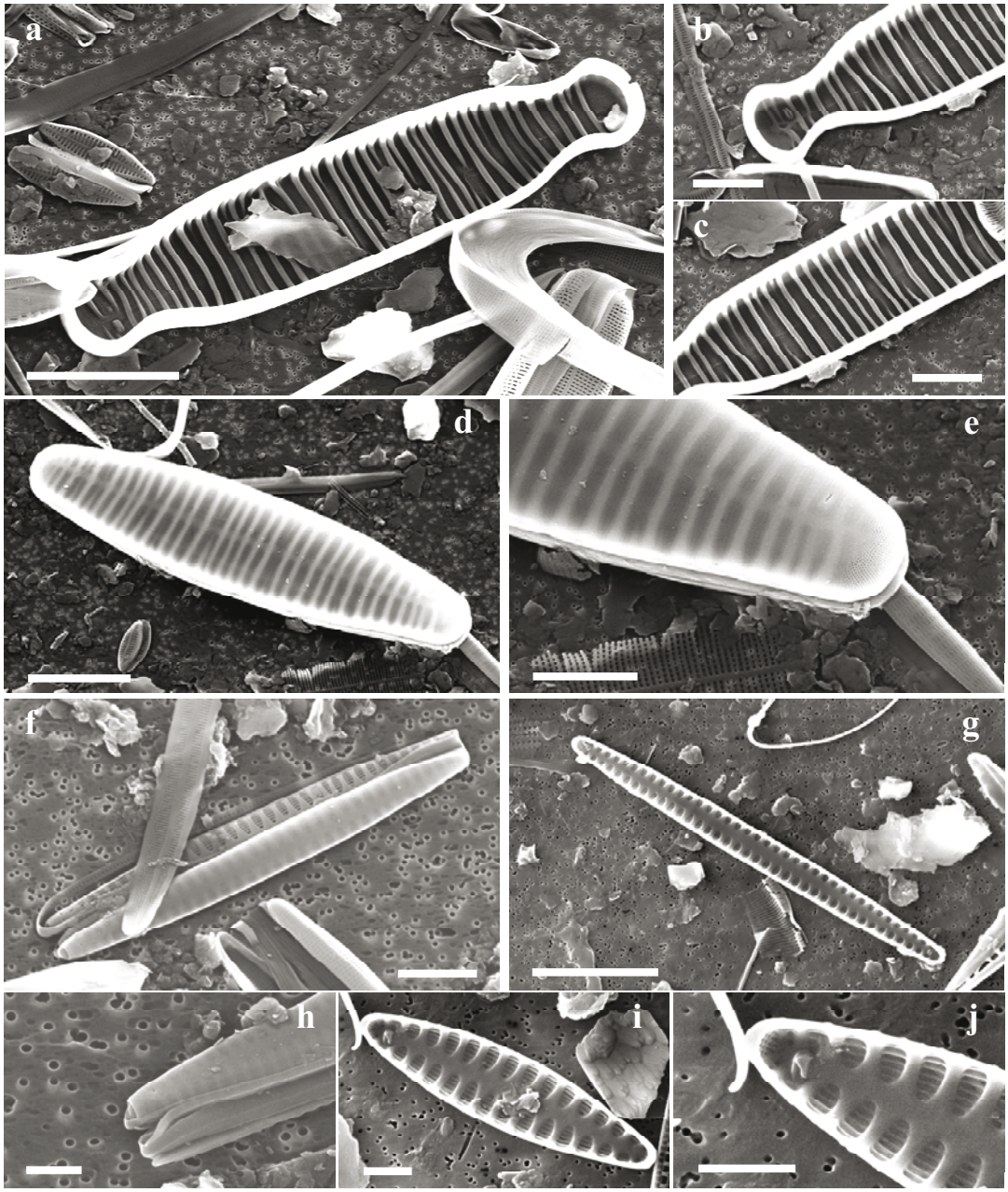

Figure 2. **a–c**= *Diatoma anceps*, SEM. **a**= Internal valve view. **b**= Internal view of the apices with apical pore fields and a rimoportula. **c**= Internal valve view showing uniseriate striae, and transapical costae irregularly spaced. **d–e**= *Diatoma vulgare*, SEM. **d**= External valve face. **e**= External apices view; apical pore field and a single rimoportula externally opened by a transapically oriented slit are visible. **f–j**= *Tabularia tabulata*, SEM. **f**= External valve face. **g**= Internal valve face. **h**= External valve face with a well-pronounced mantle, biseriate striae occluded by a cribra and an apical pore fields. **i**= Internal valve face. **j**= Internal apex view with the apical pore fields and a labiate process. Scale bars: a, d, g = 10 µm; b, c, e, f = 5 µm; h–j = 2 µm.

uniseriate, consisting of transapically elongated areolae occluded by cribra (Figures 3d and 3e); basal pole shows small round areolae (Figure 3e). Striae coarser near the base, becoming finer close to the head pole (Figures 3d and 3e). Labiate process present internally to each apex (Figure 3b), opening externally in slitlike fissure well visible at head pole (Figure 3d). Valvocopula exhibiting a penetrating internal septum on the head pole (Figure 3c), and transapical costae are visible in internal valve face (Figures 3a and 3b).

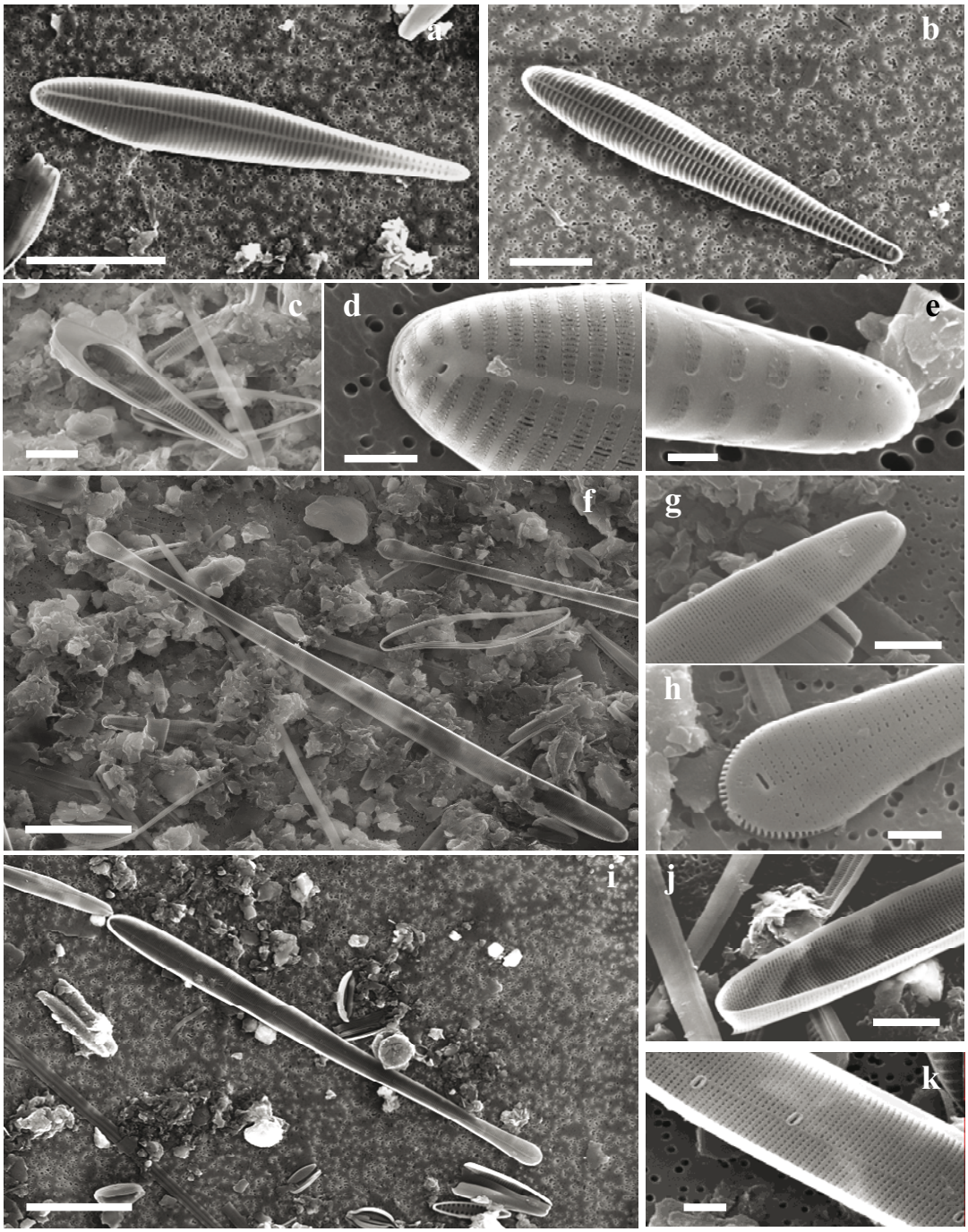

Figure 3. **a–e=** *Licmophora abbreviata*, SEM. **a=** External view showing transapical striae. **b=** Internal valve view with sternum. **c=** Valvocopula with an internal septum on the head pole. **d=** External head pole showing a slitlike labiate process transapically oriented. **e=** External foot pole with striae and small round areolae. **f–k=** *Licmophora flabellata*, SEM. **f=** External valve face. **g=** External head pole with a pronounced mantle and uniseriate transapical striae. **h=** External foot pole with striae and slitlike labiate process. **i=** Internal valve view with a narrow sternum. **j=** Internal head pole showing the sternum with slitlike rimoportula. **k=** Internal valve showing rimoportulae. Scale bars: a, f, i = 20 µm; b, c = 10 µm; g, j = 5 µm; d, h, k = 2 µm; e = 1 µm.

Notes: *Licmophora abbreviata* is an erect form attached to the substrata by a gelatinous peduncle extruded by the foot pole apical pore field. It forms colonies with a ramified pattern, in which one or more cells are attached to branches of the main stalk. *Licmophora abbreviata* represents one of the most abundant *Licmophora* species on *Eudendrium racemosum*, occurring from autumn to spring, with higher density in spring, mainly in the upper part of the hydroid colony under the polyps.

Licmophora flabellata (Carmichael ex Greville) C.Agardh emend Sar & Ferrario (1990) (Figures 3f–3k)

Bas.: *Exilaria flabellata* Ehrenberg (1832).

Refs: Sar and Ferrario, 1990; Kützing, 1844; Van Heurck, 1880–1885; De Toni, 1892; Peragallo and Peragallo, 1897–1908; Boyer, 1927; Hustedt, 1933; Geissler et al., 1963; Honeywill, 1988; Lobban et al., 2011.

Meas.: AA: 94–120 μm; TA: 4–8 μm; TS in 10 μm: 30 near basal pole, 32–35 near head pole.

Description: Cells heteropolar, clavate in valve view (Figures 3f and 3i). Valve narrow with a blunt head pole (Figure 3g) and a round capitate foot pole (Figure 3h). Valve surface slightly convex with a pronounced mantle near the head pole (Figures 3g and 3j) becoming shorter close to the foot pole (Figure 3h). Sternum narrows lacking of central area (Figures 3i and 3k). Transapical striae uniseriate, consisting of circular areolae (Figures 3g and 3h). Internally, one or more rimoportulae can be present near the sternum (Figures 3i and 3k).

Notes: *Licmophora flabellata* is an erect form. It forms typically fan-shaped colonies, attaching to the substratum through a single mucilaginous stalk extruded by the basal pole. It is one of the most abundant *Licmophora* species colonizing *Eudendrium racemosum*, occurring from autumn to spring, with higher density in spring, mainly in upper part of colony under the polyp.

Licmophora cf. ***communis*** (Heiberg) Grunow in Van Heurck (1880–1885) (Figures 4a–4c)

Bas.: *Podosphenia communis* Heiberg (1863).

Refs: Van Heurck, 1880–1885; Peragallo and Peragallo, 1897–1908; Hustedt, 1933; Okuno, 1970; Makarova and Guslyakov, 1984; Poulin et al., 1984b; Honeywill, 1988.

Meas.: AA: 48–60 μm; TA: 6–10 μm; TS in 10 μm: 27 near basal pole, 35 near head pole.

Description: Cells heteropolar, clavate in valve view (Figures 4a and 4b) and wedge-shaped in girdle view (Figure 4b). Sternum is narrow and discernible from the internal valve face (Figure 4a). Valve surface slightly convex with a pronounced mantle near the round head pole, becoming shorter close to the foot pole (Figure 4a). Transapical striae uniseriate, consisting of small areolae (Figures 4b and 4c). Internally, transapical costae are slightly bigger and closer to the basal pole than the head pole (Figure 4a). Valvocopula exhibiting a well-developed internal septum at the head pole (Figure 4b).

Notes: *L.* cf. *communis* is an erect form attached to the substrata by a gelatinous stalk extruded by the foot pole apical pore field. Morphology of *L. communis* colonies resembles those of *L. abbreviata*. It is well represented in the *Eudendrium racemosum* colony, occurring from autumn to spring, with high density in spring, mainly in the upper parts of colony under the polyps.

Remarks on taxonomy: Our specimens of *L. communis* agree in almost all respects with the original diagnosis and illustrations of Grunow in Van Heurck (1880–1885) and those in the literature (Hustedt, 1933; Honeywill, 1988), except for the number of the transapical striae, which is greater in our specimens. In particular, Van Heurck and Hustedt found 11–13 striae near the basal pole, while near the head pole the number of striae was 27–28 (Van Heurck, 1880–1885) and 28 (Hustedt, 1933). Honeywill (1988) also found a smaller number of striae than in our specimens (24 near head pole, 17 near basal pole). For this inconsistency, we prefer to add the "cf." abbreviation to make our identification more accurate. *L. communis* can be compared with *L. paradoxa* (Lyngbye) C.Agardh, having a similar valve shape but differing in the valve measures. Indeed, *L. paradoxa* can reach a length and width greater than *L. communis* (Honeywill, 1988; Hustedt, 1933; Van Heurck, 1880–1885). Moreover, the 2 species differ in the ornamentation on the external and internal valve face: *L. paradoxa* shows delicate transapical striae (Hustedt, 1933) and longitudinal thickenings on internal valve face (Honeywill, 1988), which are missing in *L. communis* (Figure 4c).

Licmophora reichardtii (*reichardti*) Grunow in Van Heurck (1880–1885) (Figures 4d and 4e)

Refs: Van Heurck, 1880–1885; De Toni, 1892; Peragallo and Peragallo, 1901; Hustedt, 1933.

Meas.: AA: 127 μm; TA: 14–15 μm; TS in 10 μm: 18–20.

Description: Cells heteropolar, clavate in valve view (Figure 4d). Valve outline linear or slightly undulate with a constriction at about 2/3 of the valve towards the lanceolate head pole (Figure 4d). Foot pole is rounded (Figure 4e). Sternum narrows (Figure 4e). Transapical striae uniseriate, consisting of transapically developed areolae occluded by hymens (Figure 4e).

Notes: *L. reichardtii* is an erect form attached to the substrata by a mucilaginous stalk secreted from the foot pole; it occurred only sporadically in the *Eudendrium racemosum* colony.

Remarks on taxonomy: Our specimens of *L. reichardtii* agree in all respects with the diagnosis and illustrations in the literature (Van Heurck, 1880–1885; De Toni, 1892; Peragallo and Peragallo, 1901; Hustedt, 1933). By Van Heurck (1880–1885), this species was reported as *L. juergensii* var. *constricta* (pl. XLVII, figs. 4, 5), and

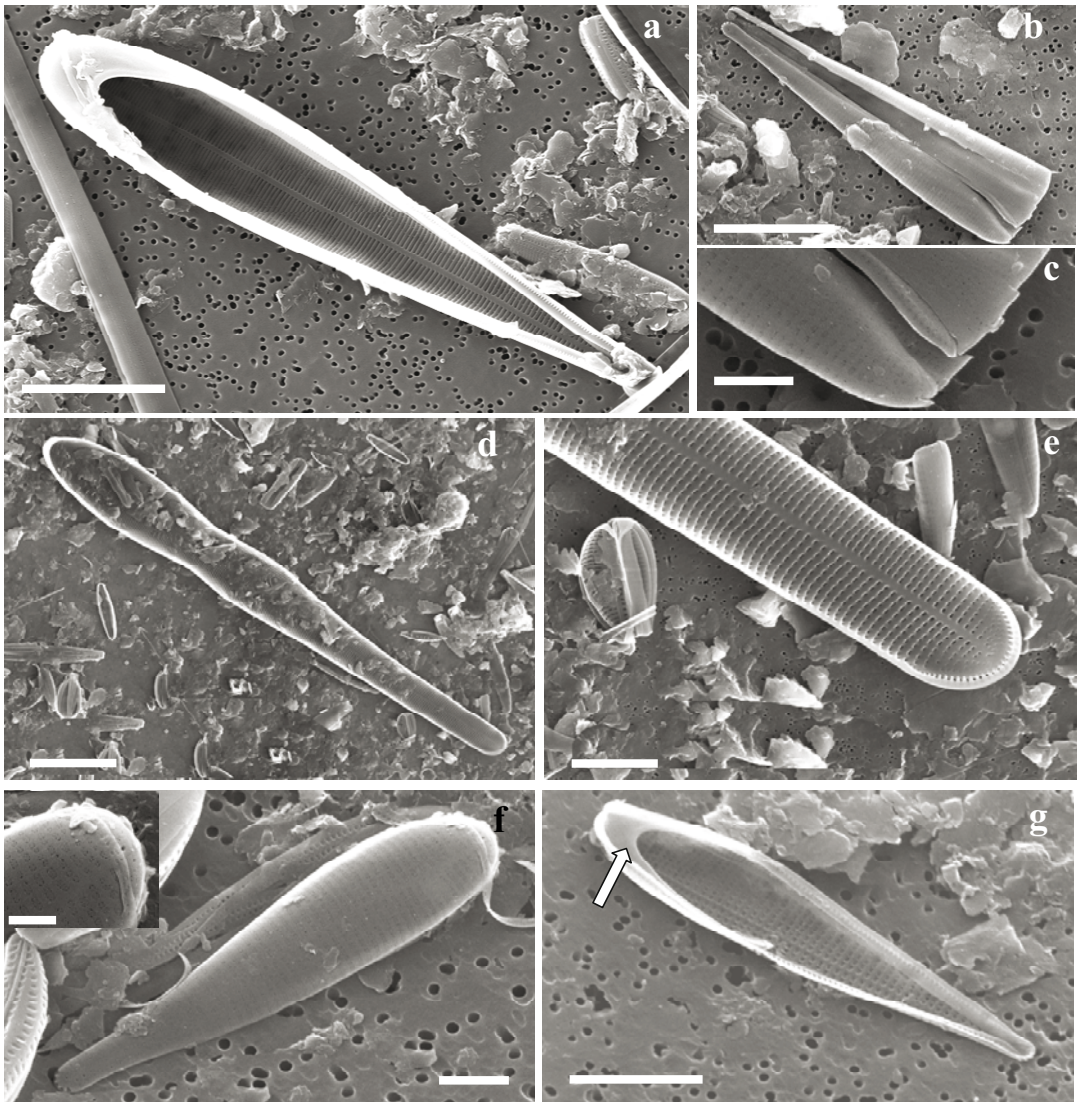

Figure 4. **a–c=** *Licmophora* cf. *communis*, SEM. **a=** Valvocopula with a well-developed internal septum. **b=** Cell in girdle view. **c=** Focus on girdle view of the head pole. **d–e=** *Licmophora reichardtii*, SEM. **d=** External valve face showing a constriction on the outline. **e.** External foot pole with uniseriate transapical striae. **f–g=** *Licmophora* cf. *dalmatica*, SEM. **f=** External valve view with narrow sternum (magnification on the areolae, scale bar = 1 µm). **g=** Valvocopulae showing septa (arrow). Scale bars: d = 20 µm; a, c = 10 µm; e, g = 5 µm; b, f = 2 µm.

it can be compared with *L.* (*juergensii* var. ?) *constricta* Grunow in Van Heurck (1880–1885, pl. XLVII, fig. 6) for its resemblance in the valve shape, even if there are differences: *L. reichardtii* is more transapically constricted and longer than *L. constricta*.

Licmophora cf. ***dalmatica*** (Kützing) Grunow (1867) (Figures 4f and 4g)

Bas.: *Rhipidophora dalmatica* Kützing (1844).

Refs: Grunow, 1867; Van Heurck, 1880–1885; De Toni, 1892; Peragallo and Peragallo, 1901; Boyer, 1927; Hustedt, 1933; Honeywill, 1988.

Meas.: AA: 11-44 µm; TA: 2-6 µm; TS in 10 µm: 30 near basal pole, 35 near head pole.

Description: Cells heteropolar, clavate in valve view (Figure 4f), showing a narrow sternum (Figure 4f). Transapical striae monoseriate with quadrangular areolae occluded by cribra (Figure 4f, magnification). Valvocopula exhibiting a well-developed internal septum at the head pole (Figure 4g, arrow).

Notes: *L.* cf. *dalmatica* is an erect form attached to the substrata with a gelatinous peduncle secreted by a foot pole; it occurred only occasionally from autumn to spring, mainly in the upper part of the *Eudendrium racemosum* colony.

Remarks on taxonomy: Specimens described in the literature agree with our specimens, except for Honeywill

(1988), who found a lower number of transapical striae (23 near basal pole, 29 near head pole) than in our samples. Moreover, other authors in the literature (see references above) mention only a cumulative number of transapical striae with a maximum of 32 (Hustedt, 1933). Therefore, "cf." has been added in the text to support these differences.

Striatellales

Striatellaceae

Grammatophora C.G.Ehrenberg

***Grammatophora angulosa* (*angulata*)** Ehrenberg (1840) (Figures 5a and 5b)

Refs: Ehrenberg, 1840; Van Heurck, 1880–1885; De Toni, 1892; Peragallo and Peragallo, 1897–1908; Boyer, 1927; Hustedt, 1933; Poulin et al., 1984b.

Meas.: AA: 25–27 µm; TA: 4–6 µm; TS in 10 µm: 17–22.

Description: Valves linear with round apices in valve view, square to rectangular in girdle view (Figure 5a); sternum indistinct (Figure 5b). Transapical striae are uniseriate, consisting of rounded areolae, which continue down the mantle, stopping before the valve edge (Figure 5a). Areolae also continue around the apices below the apical pore fields (Figure 5b). Girdle well developed and consisting of several copulae with single row of small pores. Valvocopula is closed, with prominent areas of transapically elongate areolae at the apices of the frustule (Figure 5a, arrow). Strongly undulate septae are visible in the girdle view (Figure 5a).

Notes: *Grammatophora angulosa* is an erect form attached to the substrata through a mucilaginous pad secreted from the apical pore field. Cells are attached to each other by the opposite apical pore fields forming zigzag colonies. *G. angulosa* occurred all year round with higher abundances from autumn to winter, mainly in the central and apical part of the *Eudendrium racemosum* colonies.

Grammatophora marina (Lyngbye) Kützing (1844) (Figures 5c–5g)

Bas.: *Diatoma marinum* Lyngbye (1819).

Refs: Kützing, 1844; Smith, 1856; De Toni, 1892; Van Heurck, 1880–1885; Peragallo and Peragallo, 1897–1908; Boyer, 1927; Hustedt, 1933; Hasle, 1973; Karayeva and Dzhafarova, 1987; Ricard, 1987; Gleser et al., 1988; Karayeva and Dzhafarova, 1988.

Meas.: AA: 17–32 µm; TA: 4–5 µm; TS in 10 µm: 12–26.

Description: Valves linear, slightly widened in the middle with round apices in valve view (Figure 5d), square to rectangular in girdle (Figure 5c). Sternum indistinct, lacking a central area (Figure 5d). Transapical striae are uniseriate, consisting of roundish areolae, which continue down the mantle, stopping before the valve edge (Figure 5c). Areolae also continue around the apices below the apical pore fields (Figures 5c, arrow; 5g). Apical pore fields are well developed through the surface of the poles (Figure 5f, arrow). Girdle well developed and consisting of several copulae with single row of small pores (Figure 5c). Valvocopula is closed, with prominent areas of transapically elongate areolae at the apices of the frustule (Figures 5c, arrow; 5d; 5g, arrow). Internally, valvocopula bears 2 undulate septae delimiting a single central opening (Figure 5e), which are visible in the girdle view (Figure 5c).

Notes: *Grammatophora marina* is an erect form attached to the substrata through a mucilaginous pad secreted from the apical pore field. It forms zigzag colonies, where cells are attached to the opposite apical pore fields. *G. marina* occurred all year round with higher abundances from autumn to winter, mainly in the upper part of the colony.

Toxariales

Toxariaceae

Toxarium J.W.Bailey

Toxarium undulatum J.W.Bailey (1854) (Figures 5h–5j)

Refs: Pelletan, 1889; Cupp, 1943; Round et al., 1990; Hasle and Syvertsen, 1996; Kooistra et al., 2003.

Meas.: AA: 380–430 µm; TA: 8–9 (middle), 4–5 (apex) µm; TS in 10 µm: 10–12.

Description: Cells needle-like and very long in valve view (Figure 5h). Valve face flat with smooth or undulating margins, slightly expanded in the center and in both apices (Figures 5i and 5j). Mantle and valvocopula are narrow (Figure 5i). Central area absent (Figure 5j). Circular areolae scattered over much of the valve face and forming well defined longitudinal rows along the edge of the valve (Figure 5i).

Notes: *T. undulatum* live intermingled on other epiphyte or sediment that occur on the colony of *Eudendrium racemosum* with low densities all year round. It was distributed in the central and apical part of the colony.

3.2. Biraphid diatoms

Bacillariales

Bacillariaceae

Nitzschia A.H.Hassall

Nitzschia longissima (Brébisson in Kützing) Grunow (1862) (Figures 6a–6f)

Bas.: *Ceratoneis longissima* Brébisson ex Kützing (1849).

Refs: Grunow, 1862; Van Heurck, 1880–1885; Peragallo and Peragallo, 1897–1908; Hasle, 1964; Marion et al., 1986; Poulin et al., 1990; Hasle and Syvertsen, 1996.

Meas.: AA: 140–282 µm; TA: 5–8 µm; TS in 10 µm: 34–39; fibulae in 10 µm: 5–8.

Description: Cells lanceolate, slightly curved in valve view (Figures 6a and 6d). Valves straight and needle-like, expanded centrally in the valve view (Figures 6a, 6b, 6d, and 6e). Valve face almost flat with a narrow mantle (Figures 6b and 6c). Raphe system eccentric and placed on a prominent keel, fibulate (Figures 6a, 6b, 6d, and 6f).

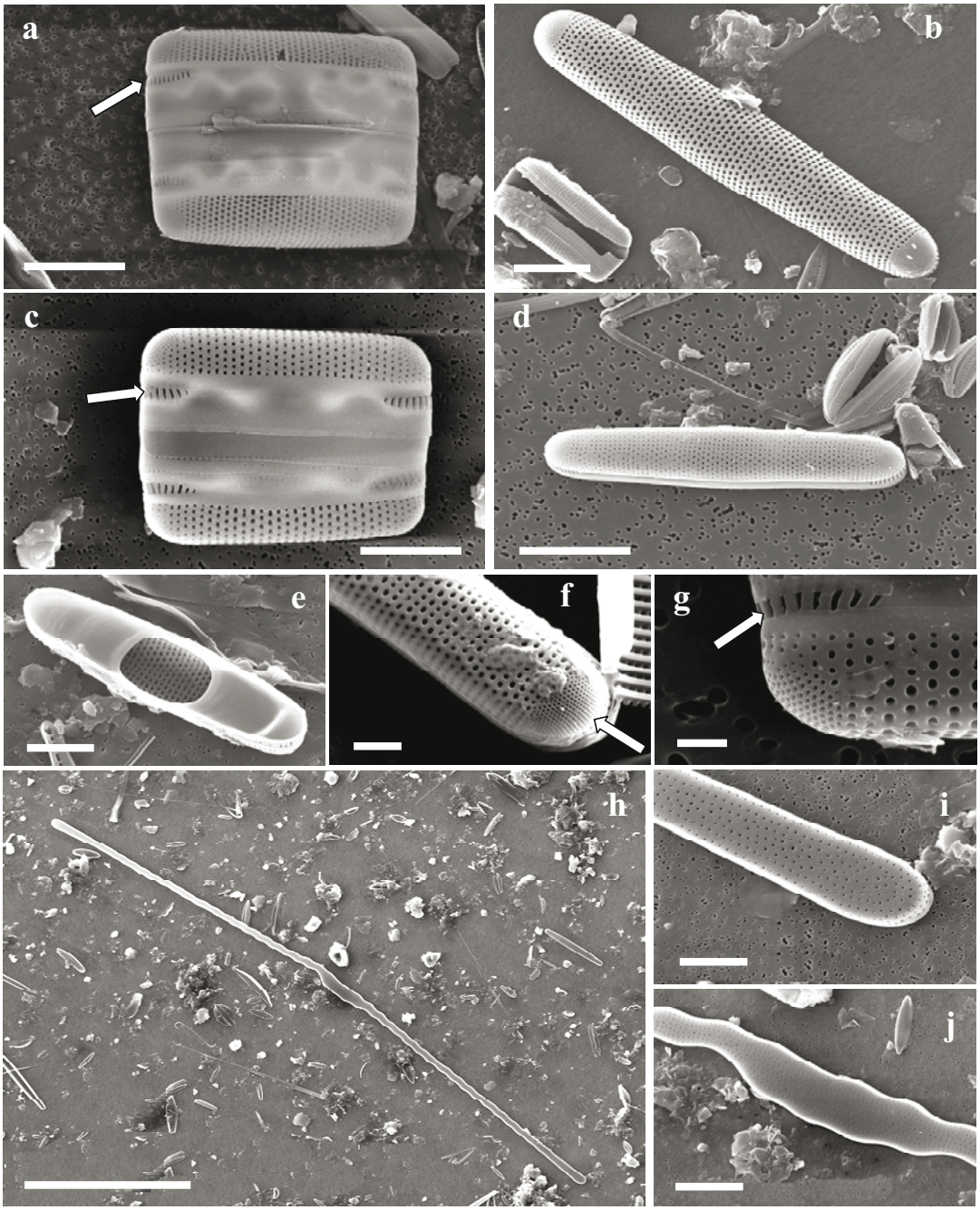

Figure 5. a–d= *Grammatophora angulosa*, SEM. **a=** Girdle view with irregularly wavy septa and transapically elongated areolae near the poles (arrow). **b=** Valve view with uniseriate transapical striae and apical pore fields. **c–g=** *Grammatophora marina*, SEM. **c=** Girdle view with irregularly wavy septa and transapically elongated areolae near the poles (arrow). **d=** Valve view with uniseriate transapical striae and apices with apical pore fields. **e=** Internal valve view occluded by septa that delimit a single central opening. **f=** External apex view with transapical striae and apical pore fields (arrow). **g=** Girdle view of the apex with area with transapically elongate areolae on the valvocopula (arrow). **h–j=** *Toxarium hennedyanum*, SEM. **h.** Valve face. **i.** Valve apex with areolae scattered over much of the valve face and longitudinal striae on the edge. **j=** Valve face showing expanded central area. Scale bars: h = 100 µm; a, d, j = 10 µm; b, c, e, i = 5 µm; f = 2 µm; g = 1 µm.

Internally, fibulae are irregularly distanced to form the canal raphe (Figure 6e). Central raphe endings are simple (Figures 6b and 6c), while externally the terminal fissures are hooked towards proximal side (Figure 6c). Transapical striae are equidistant, parallel, and uniseriate with small rounded areolae (Figure 6e).

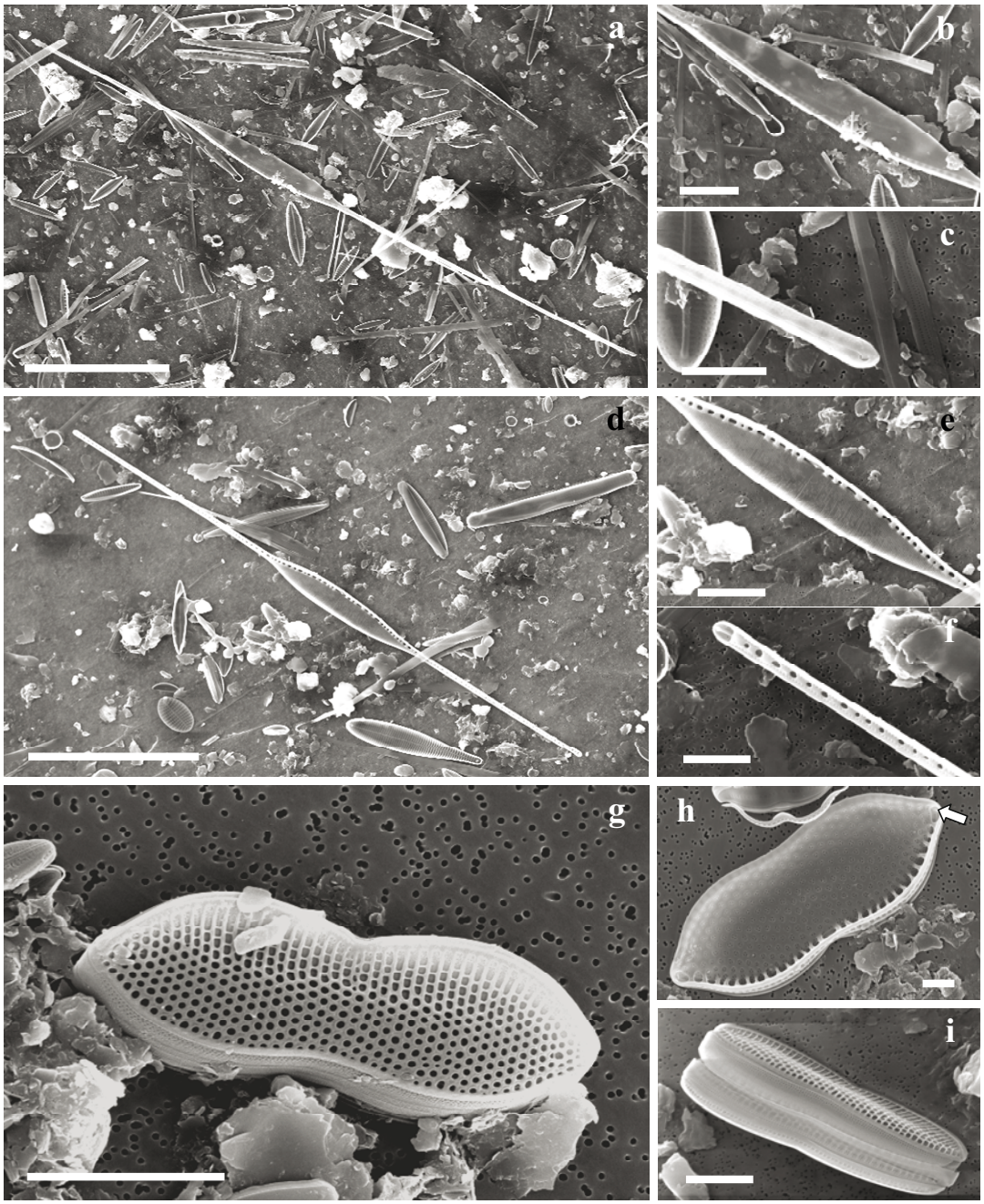

Figure 6. **a–f=** *Nitzschia longissima*, SEM. **a=** External valve face. **b=** External valve central showing internal fibulae and narrow mantle. **c=** External apical valve with external raphe hooked fissure. **d=** Internal valve face. **e=** Internal central valve with transapical striae, canal raphe, and fibulae. **f=** Internal valve ending showing the canal raphe closed by fibulae. **g–i=** *Psammodictyon mediterraneum*, SEM. **g=** External valve face. **h=** Internal valve view with eccentric raphe bearing on a keel and very small helictoglossae (arrow). **i=** Girdle view with singular band ornate by simple poroid. Scale bars: a, d = 50 µm; b, e, g = 10 µm; c, f, i = 5 µm; h = 2 µm.

Notes: *Nitzschia longissima* is a motile form that lives on the colony of *Eudendrium racemosum* with low densities all year round. It was distributed in all colony parts.

Bacillariales

Bacillariaceae

Psammodictyon D.G.Mann in F.E.Round, R.M.Crawford & D.G.Mann

Psammodictyon mediterraneum (Hustedt in A.Schmidt) Mann in Round, Crawford & Mann (1990) (Figures 6g–6i)

Refs: Round et al., 1990; Poulin et al., 1990.

Meas.: AA: 12–32 µm; TA: 5–10 µm; TS in 10 µm: 12–20; fibulae in 10 µm: 10–13.

Description: Cells panduriform with apiculate apices in valve view (Figures 6g and 6h), rectangular shape in girdle view (Figure 6i). Valve face is depressed on one side toward raphe system (Figures 6g and 6i), and it shows a narrow mantle lacking areolae (Figure 6i). Raphe submarginal, keeled and constituted internally by simple rib-like fibulae (Figure 6h). Internally, central raphe endings terminate in very small helictoglossae (Figure 6h, arrow). Striae consisting of quadrangular to roundish loculate areolae disposed in quincunx internally occluded by cribra (Figure 6h) and externally opened by a large foramen (Figure 6g). Girdle is formed of open bands; the most advalvar band generally bears 2 to several rows of small round poroids (Figure 6i).

Notes: *Psammodictyon mediterraneum* is a motile form present on the *Eudendrium racemosum* colony all year round, with low densities. Slightly higher abundance was observed in spring and summer. It was distributed mainly in the basal and central part of the *E. racemosum* colony.

Bacillariales

Bacillariaceae

Tryblionella W.Smith

Tryblionella marginulata var. ***subconstricta*** f. ***minuta*** (Grunow) Poulin in Poulin, Bérard-Therriault & Hamilton (1990) (Figures 7a–7d)

Bas.: *Nitzschia marginulata* var. *subconstricta* f. *minuta* Grunow in Cleve & Grunow (1880).

Refs: Poulin et al., 1990; Akbulut, 2003.

Meas.: AA: 20–46 µm; TA: 4–10 µm; TS in 10 µm: 30–44; fibulae in 10 µm: 14–16.

Description: Cells panduriform in valve view with rostrate apices (Figures 7a, 7b, and 7d). Raphe-sternum is hardly visible (Figure 7c) and strongly eccentric (Figures 7a and 7c). Valves surface undulate, sloping down in a scarcely developed mantle (Figure 7c). Striae uniseriate, parallel in the valve center slightly radial close to the apices, consisting of circular areolae (Figure 7c). Internally, fibulae of the raphe system are unequally distributed with a central larger interspace near the central nodule (Figure 7d). The central external raphe endings are very close together (Figure 7c, arrow). Internal central and distal raphe endings terminate in helictoglossae (Figure 7d, arrow). Girdle consisting of several open bands (Figures 7a and 7c).

Notes: *Tryblionella marginulata* var. *subconstricta* f. *minuta* is a motile form occurring with low abundances on the *Eudendrium racemosum* colony. It was distributed preferentially in the central and apical part of the colony with the other motile forms.

Mastogloiales

Mastogloiaceae

Mastogloia Thwaites ex W.Smith

Mastogloia undulata Grunow (1860) (Figures 7e–7g)

Refs: Grunow, 1860; Cleve, 1885; Peragallo and Peragallo, 1897–1908; Hustedt, 1933; Podzorski and Håkansson, 1987.

Meas.: AA: 31–32 µm; TA: 13–14 µm; TS in 10 µm: 11.

Description: Cells lanceolate in valve view with rostrate apices (Figure 7e). Raphe-sternum slightly dilated at center. Externally, raphe consists of 2 sinuous slits with 2 flaps emerging centrally from the sternum (Figures 7e, arrow; 7g), ending centrally in simple pores deflected in the same direction and distally in terminal fissures hooked toward the same side (Figures 7e–7g). Transapical striae are parallel at center and slightly radiate at poles, forming an irregular longitudinal pattern, and composed of uniseriate rows of areolae (Figure 7e). The ornamentation of the external valve face is composed by irregularly sized quadrangular areolae (Figures 7e–7g). Mantle is scarcely developed, lacking areolae (Figures 7e and 7f). Girdle consisting of a valvocopula with partectal pores (Figure 7e).

Notes: *Mastogloia undulata* is a motile form, occurring only occasionally on the *Eudendrium racemosum* colony. It was distributed preferentially in the central and apical parts of the colony with the other motile forms.

Naviculales

Berkeleyaceae

Berkeleya Greville emends Cox

Berkeleya rutilans (Trentepohl ex Roth) Grunow (1880) (Figures 7h–7j)

Bas.: *Conferva rutilans* Trentepohl ex Roth (1806).

Refs: Grunow, 1880; Patrick and Reimer, 1966; Cox, 1977, 1981; Navarro, 1982a; Cardinal et al., 1984; Lobban, 1984; Makarova and Akhmetova, 1986; Gleser et al., 1988; Watanabe, 1988.

Meas.: AA: 11–20 µm; TA: 2–4 µm; TS in 10 µm: 31–46.

Description: Cells linear to linear-lanceolate in valve view with rounded apices (Figures 7h–7j). Valve face a little wider, sometimes curves quickly into the mantle (Figure 7h). Raphe slits are short, straight, and about 1/3 of the length of the valve from each apex, characterized by central and apical endings deflected in the same direction (Figures 7h and 7i). Transapical striae uniseriate, almost perpendicular to the axial line and consisting of circular areolae (Figure 7h). Immediately adjacent to the central sternum, the areolae are much wider transapically than elsewhere (Figures 7h and 7i). Internally, transapical interstriae are visible in all valve faces (Figure 7j). Girdle consists of few open bands, each of which bear 2 rows of circular poroids (Figure 7i).

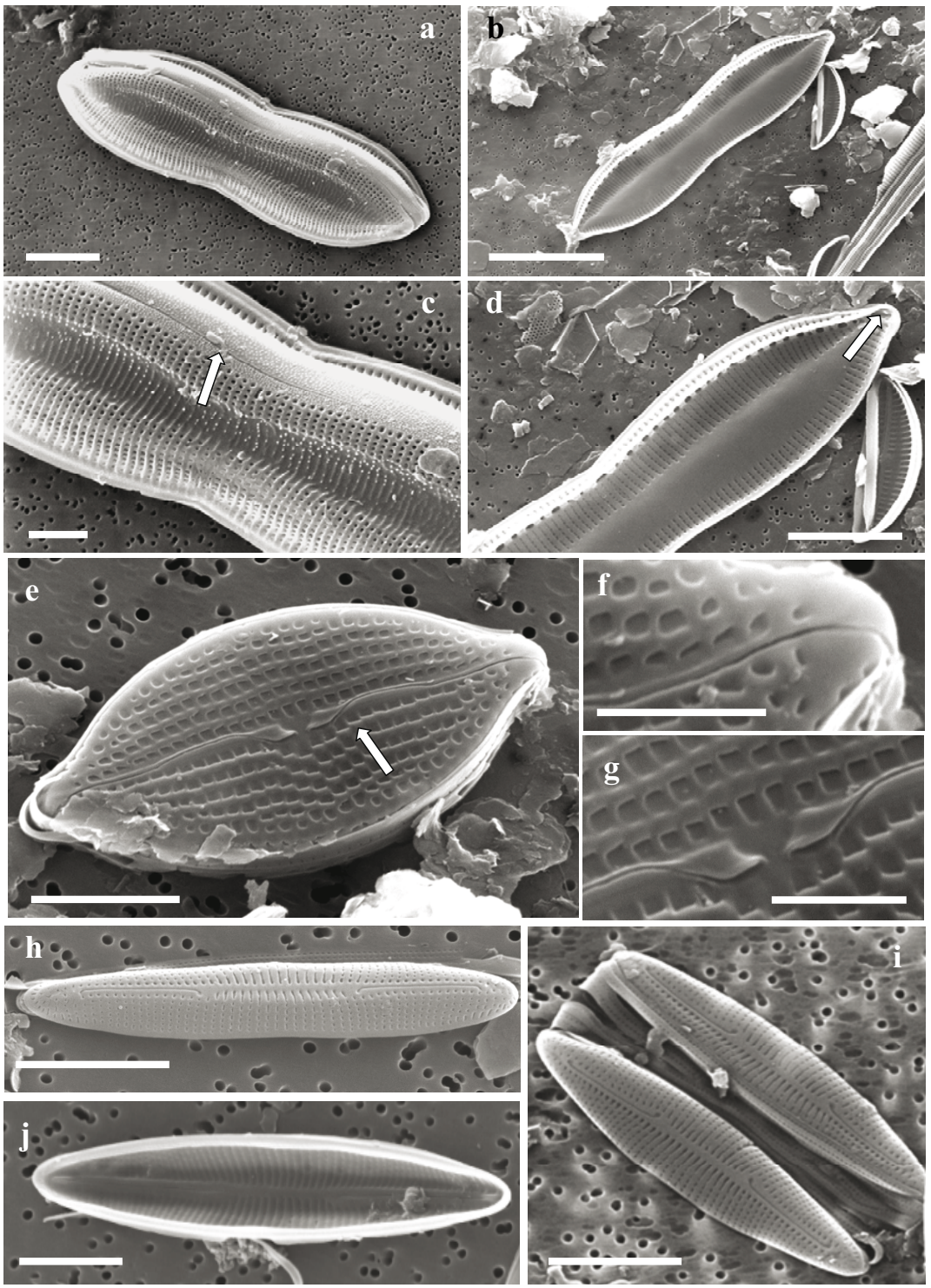

Figure 7. a–d= *Tryblionella marginulata* var. *subconstricta* f. *minuta*, SEM. **a**= External valve face. **b**= Internal valve face. **c**= External view of a central valve with uniseriate parallel striae and central raphe fissure (arrow). **d**= Internal valve view with transapical striae, and raphe system with fibulae and helictoglossae (arrow). **e–g**= *Mastogloia undulata*, SEM. **e**= External valve face with sinuous raphe and flaps (arrow). **f.** External apical valve face focus on hooked terminal raphe fissure. **g**= Central valve face focus on central raphe endings and flaps. **h–j**= *Berkeleya rutilans*, SEM of a tube-dwelling form. **h**= Valve face with straight and short raphe slits. **i.** Cell open, 2 valves and girdle bands are visible. **j**= Internal face with straight raphe slits and transapical interstriae. Scale bars: b = 10 µm; a, d, e, h, i, j = 5 µm; c, f, g = 2 µm.

Notes: *Berkeleya rutilans* is a tube-dwelling form, living in mucilage tubes forming turfs over substrata. It occurred all year round with low densities without a clear preference for any part of *Eudendrium racemosum* colony; annual peak occurred in early summer.

Naviculales

Diploneidaceae

Diploneis (C.G.Ehrenberg) P.T.Cleve

Diploneis cf. ***stroemi*** Hustedt (1937) (Figures 8a and 8b)

Refs: Hustedt, 1933; Hendey, 1964; Cardinal et al., 1984; Simonsen, 1987; Witkowski et al., 2000.

Meas.: AA: 46–47 µm; TA: 14–15 µm; TS in 10 µm: 8.

Description: Cells panduriform in valvar view with rounded apices and a convex valve face (Figure 8a). Raphe-sternum broad with a roundish central area and lateral areas, about 1/3 of the valve width in size, bearing longitudinal canals externally opening in a single apical row of roundish areolae (Figure 8b). Externally the raphe slits are straight with coaxial central simple pores (Figure 8b). Terminal raphe fissures are deflected (Figure 8a). Transapical striae perpendicular to the raphe-sternum in the center of the valve and radial toward the apices (Figure 8a) consisting of loculate (Figure 8b). Girdle consisting of a large valvocopula (Figure 8a, arrow).

Notes: *Diploneis* cf. *stroemi* is a motile form. It occurred all year round with low densities and with a preference for the central and apical part of the *Eudendrium racemosum* colony.

Remarks on taxonomy: Our specimens of *Diploneis* cf. *stroemi* agree in all respects with the diagnosis and illustrations in the literature (see references above); however, for the slight degradation of the striae that occurs in our samples, we prefer to add the "cf." abbreviation.

Diploneis oculata (Brébisson in Desmazières) Cleve (1894) (Figures 8c–8g)

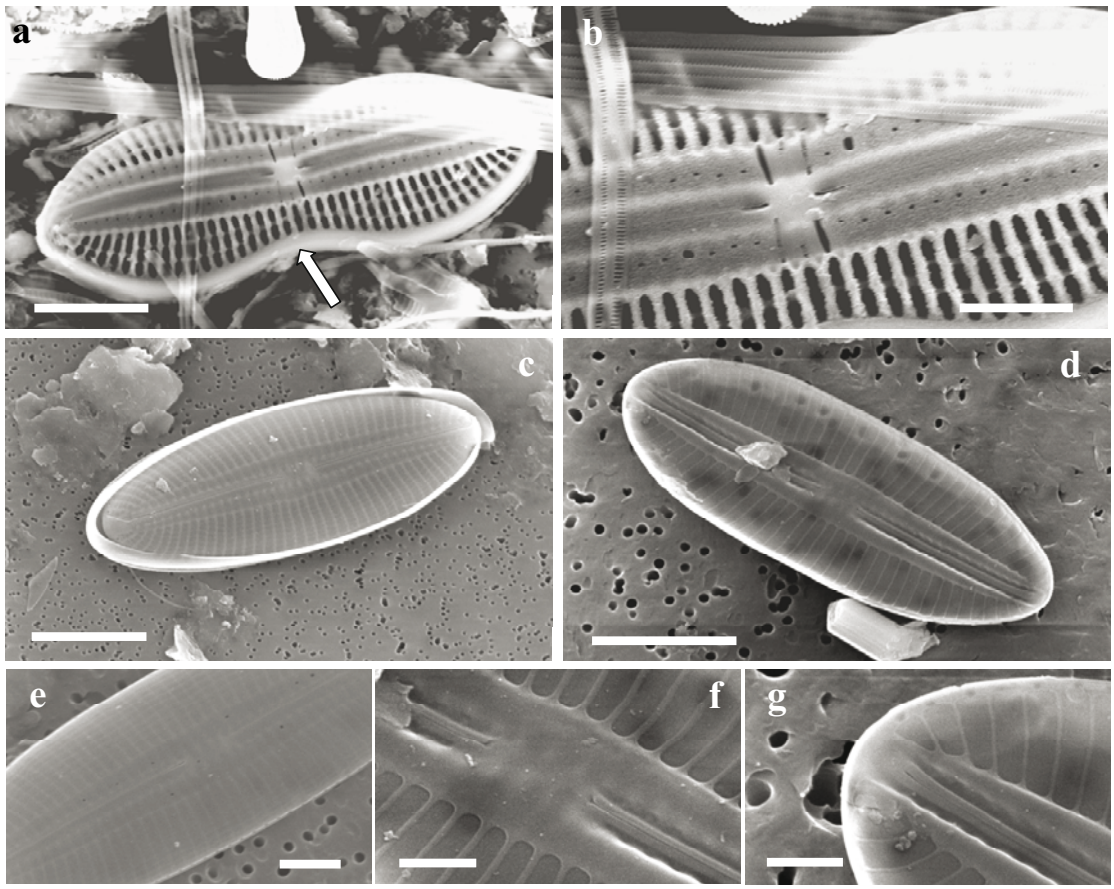

Figure 8. a–b= *Diploneis* cf. *stroemi*, SEM. **a**= Valve view showing a partial valvocopula (arrow). **b**= Central area showing coaxial central simple pore of the raphe slits. **c–g**= *Diploneis oculata*, SEM. **c**= External valve face. **d**= Internal valve face. **e**= External valve view with transapical striae perpendicular to the raphe-sternum. **f**= Internal central nodule bearing raphe endings. **g**= Internal face of the apice. Scale bars: a = 10 µm; b, c, d = 5 µm; e = 2 µm; f, g = 1 µm.

Bas.: *Navicula oculata* Brebisson in Desmazières (1854).

Refs: Cleve, 1894; Van Heurck, 1880–1885; Hustedt, 1930, 1933; Germain, 1979, 1981; Idei and Kobayasi, 1986.

Meas.: AA: 14–20 µm; TA: 5–6 µm; TS in 10 µm: 20–25.

Description: Cells elliptical to linear-elliptical in valvar view and a convex valve face (Figures 8c and 8d). Raphe-sternum broad with a roundish central area and lateral areas, about 1/5 of the valve width in size (Figures 8c and 8e), bearing longitudinal canals that are often open externally with some quadrangular areolae irregularly arranged (Figure 8f). Raphe slits straight with coaxial central simple pores (Figures 8c and 8e). Terminal raphe fissures are bent to the same side of the valve (Figure 8c). Internally, raphe is straight and bordered by raised siliceous ribs and terminate in small pores at the central nodule far from each other (Figures 8d, 8f, and 8g). Transapical striae perpendicular to the raphe-sternum in the center of the valve (Figure 8e) and radial toward the apices, consisting of loculate areolae, continuing down on the mantle, and externally occluded by complex cribra (Figures 8d, 8f, and 8g). Internally, central raphe ending and polar endings terminating in simple pores (Figures 8f and 8g). Girdle consisting of a large valvocopula and few open copulae.

Notes: *Diploneis oculata* is a motile form. It occurred all year round with low density, mainly in the central and apical part of the *Eudendrium racemosum* colony.

Naviculales

Gomphocymbelleae

Amphora C.G.Ehrenberg ex F.T.Kützing

Amphora coffeaeformis (C.Agardh) Kützing (1844) (Figures 9a–9e)

Bas.: *Frustulia coffeaeformis* C.Agardh (1827).

Refs: Kützing, 1844; Peragallo and Peragallo, 1897–1908; Helmcke and Krieger, 1953; Hustedt, 1933; Van Der Werff and Huls, 1957–1974; Anderson, 1975; Patrick and Reimer, 1975; Ehrlich, 1978; Bradbury and Blair, 1979; Archibald, 1983; Archibald and Barlow, 1983; Archibald and Schoeman, 1984; Karayeva et al., 1984; Ehrlich and Dor, 1985; Gusylakov, 1985; Bérard-Therriault et al., 1986; Cooksey and Cooksey, 1986; Dor and Ehrlich, 1987; Compère and Delmotte, 1988; Guslyakov, 1988.

Meas.: AA: 14–30 µm; TA: 4–11 µm; TS in 10 µm: 16–23.

Description: Valves asymmetrical in the apical plane and constricted near the poles with a convex dorsal margin and straight ventral margin (Figures 9a, 9b, and 9c). The dorsal valve face is wide and gently curves into the dorsal mantle. The ventral valve face is narrow and at a right angle to the ventral mantle (Figure 9d). Raphe straight and located very close to the ventral margin (Figures 9a and 9c). The raphe external fissures at the poles are strongly hooked in the same direction (Figure 9a) or straight (Figure 9e) and proximal ends are deflected to strongly deflected towards the same side (Figures 9a, 9c and 9d), simple and not dilated (Figure 9d). The dorsal striae are parallel to slightly radiate from the center toward the apices and formed by 2 rows of circular areolae interrupted by costae of similar width on the dorsal side of the valve (Figure 9d). The ventral striae are similar to the dorsal striae but are interrupted at the valve center and consist of a single transapical elongated areola (Figure 9d). Intercalary bands numerous, perforated by a single apical row of circular poroids (Figure 9b).

Notes: *Amphora coffeaeformis* has an adnate life form; it attaches to the substrata through the girdle side and is able to make small movements by the secretion of mucilage from the raphe. Occurs year round with rather high abundance, mainly from autumn to spring, without any evident preference for any part of the *Eudendrium racemosum* colony.

Amphora ovalis **var.** ***pediculus*** (Kützing) Pero (1893) (Figures 9f–9i)

Bas.: *Cymbella pediculus* Kützing (1844).

Refs: Pero, 1893; Helmecke and Krieger, 1954; Van Der Werff and Huls, 1957–1974; Karayeva and Gadzhieva, 1975; Patrick and Reimer, 1975.

Meas.: AA: 7–13 µm; TA: 2–7 µm; TS in 10 µm: 20–30.

Description: Cells appear elliptical with truncate ends in girdle view (Figure 9g). Valves asymmetrical in the apical plane with a convex dorsal margin and straight ventral margin (Figure 9h). The dorsal valve face is wide and gently curves into the dorsal mantle (Figures 9f and 9i). The ventral valve face is narrow and at a right angle to the ventral mantle (Figure 9h). Raphe is straight and located very close to the ventral margin (Figures 9g and 9h). The dorsal striae are parallel to slightly radiate from the center towards the apices and formed by a row of elongated areolae interrupted by longitudinal and costae on the dorsal side of the valve (Figures 9g; 9h, arrow). The ventral striae are similar to the dorsal but interrupted at the central valve and consist of a single transapically elongated areola occluded by hymens (Figure 9h). Dorsal side of the valve formed by numerous hyaline intercalary bands (Figures 9f and 9i).

Notes: *Amphora ovalis* var. *pediculus* is an adnate form; it lies on the substrata, where is able to make small movements through the secretion of mucilage from raphe. It occurred all year round with high densities; its annual peak occurred from autumn to early summer, without a spatial gradient over the hydroid colonies.

Naviculales

Naviculaceae

Caloneis Cleve

Caloneis alpestris (Grunow) Cleve (1894) (Figures 10a–10e)

Bas.: *Navicula alpestris* Grunow (1860).

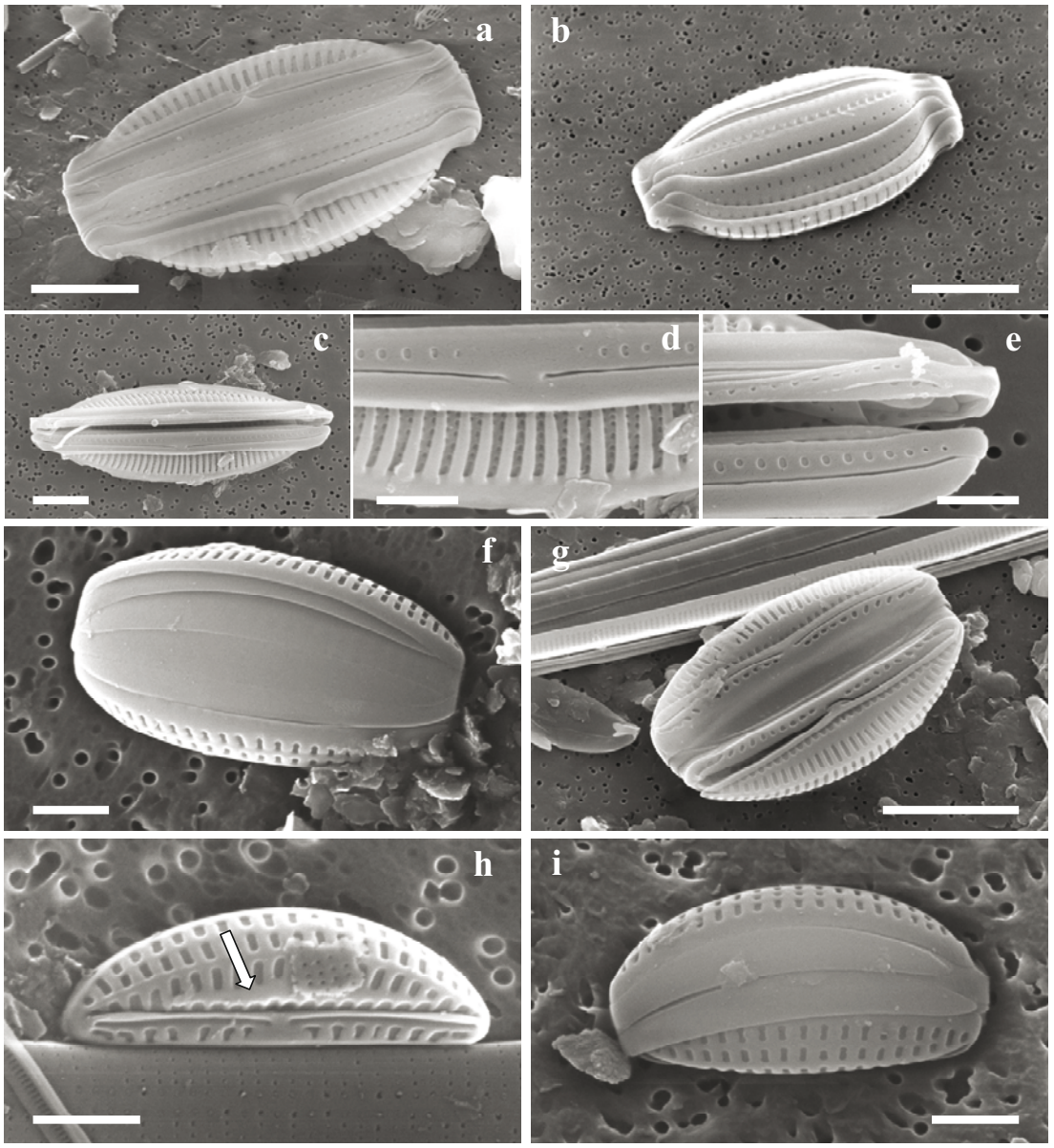

Figure 9. **a–e=** *Amphora coffeaeformis*, SEM. **a=** Girdle view of cells constricted near the poles. **b=** Dorsal valve face with apical rows of circular poroids. **c=** Ventral valves view with straight raphe fissures. **d=** Central part of cell showing proximal raphe ends simple and barely dorsally bent. **e=** Pole of the valve with straight raphe fissure. **f–i=** *Amphora* cf. *ovalis* var. *pediculus*, SEM. **f=** Dorsal side of the cell with numerous intercalary bands unpierced. **g=** Girdle view with raphe fissures. **h=** Valve view with raphe and striae consisting of a single transapically elongated areolae and costae (arrow). **i=** Dorsal side of the valve with intercalary bands. Scale bars: a–c, g = 5 µm; d, e, f, h, i = 2 µm.

Refs: Cleve, 1894; Husted, 1985.

Meas.: AA: 30–72 µm; TA: 6–10 µm; TS in 10 µm: 25–32.

Description: Cells are linear-elliptical in valve view, rectangular in girdle view (Figures 10a and 10e). Valve face flat with rounded apices sloping down in a shallow mantle (Figures 10a and 10e). Raphe-sternum narrows with 2 siliceous thickenings bordering the central area (Figure 10c). Transapical striae uniseriate, parallel in the center of the valve to slightly radial close to the apices (Figure 10a). Externally, raphe is straight, with expanded central pores ending in the central area (Figure 10c) and distal endings deflected toward the same side (Figures 10a and 10d). Internally, the straight raphe slits end coaxially at center on central nodule and distally in helictoglossae (Figure 10b). In internal valve face there is a row of areolae

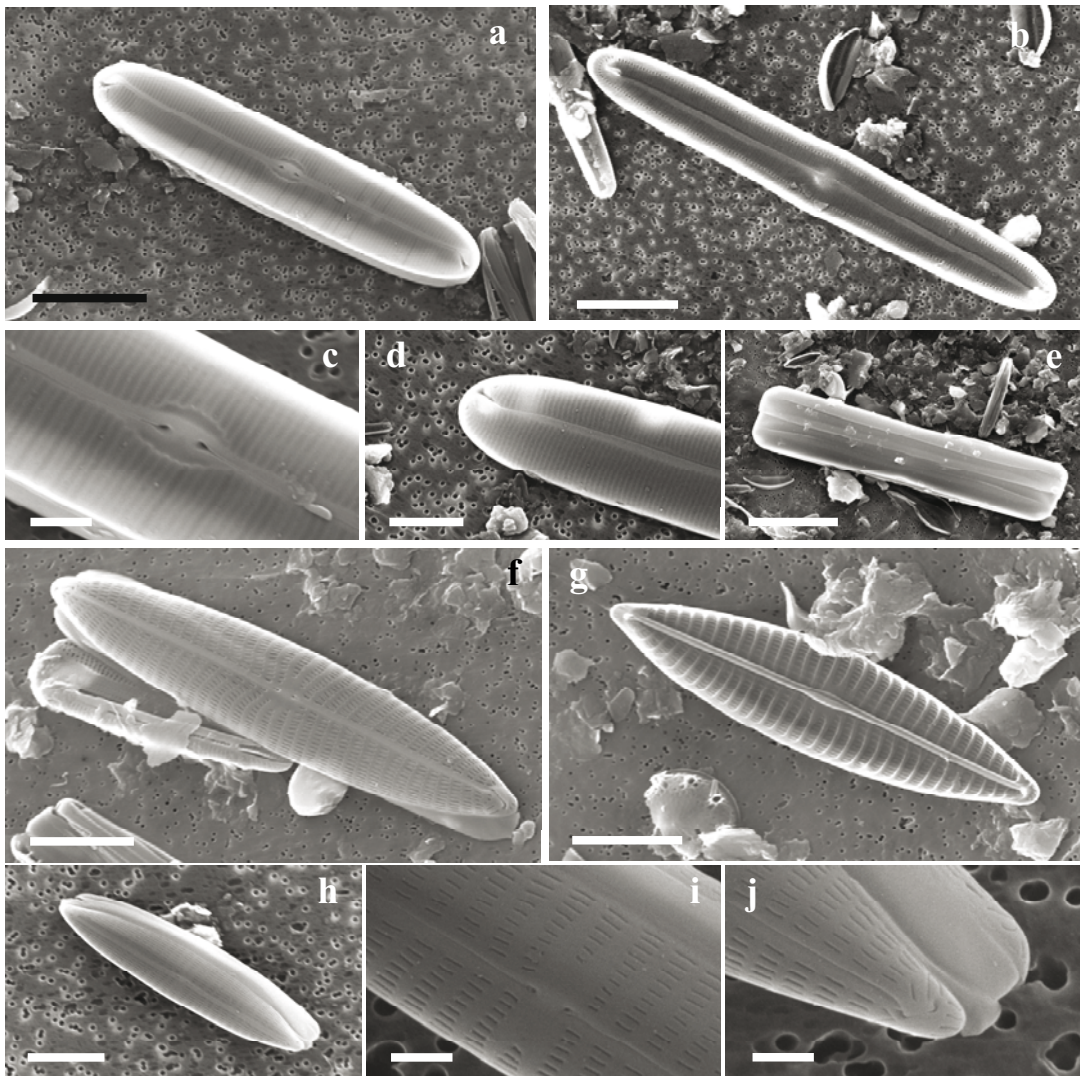

Figure 10. a–e= *Caloneis alpestris*, SEM. **a**= External valve face. **b**= Internal valve view with helictoglossae. **c**= Central area with expanded central pores of the raphe. **d**= Apical area of the external valve showing transapical striae and raphe terminal fissure deflected. **e**= Girdle valve view showing mantle and bands. **f–j**= *Navicula* cf. *consentanea*, SEM. **f**= External valve face. **g**= Internal valve view with straight raphe. **h**= Tilted view of the valve. **i**= Central part of the valve showing slightly expanded central pores of the raphe. **j.** Apical area with hooked terminal fissures of the raphe. Scale bars: e = 20 µm; a, b = 10 µm; d, f–h = 5 µm; c = 2 µm; i, j = 1 µm.

that form a circle along the edge of the valve (Figure 10b). Girdle consists of a few bands, the first of which is usually the widest (i.e. valvocopula; Figure 10e).

Notes: *Caloneis alpestris* is a motile form. It showed the highest densities from autumn to spring with a peak in winter and occurred in the *Eudendrium racemosum* colony mainly in the basal and central parts. Although it is a freshwater form, its occurrence in our samples may be explained with the presence of freshwater input near the sampling site.

Naviculales

Naviculaceae

Navicula Bory de Saint-Vincent

Navicula cf. ***consentanea*** Hustedt (1939) (Figures 10f–10j)

Refs: Hustedt, 1939; Patrick and Reimer, 1966; Simonsen, 1987.

Meas.: AA: 15–31 µm; TA: 3–7 µm; TS in 10 µm: 14–22.

Description: Cells are linear-lanceolate in valve view (Figures 10f and 10h) with rounded apices sloping down in a mantle (Figures 10f and 10h). Raphe-sternum narrow, with transapically expanded central area (Figures 10f and 10i). Raphe straight with slightly expanded central pores (Figure 10i). Distal terminal fissures hooked toward the same side (Figures 10g and 10j). Internally the raphe is straight with proximal and distal pores ending in a

raised central nodule and helictoglossa, respectively. The internal raphe-sternum is bordered over most of its length by 2 thick, narrow, and linear axial costae (Figure 10g). Transapical uniseriate striae are radial, consisting of apically elongated areolae (Figures 10f and 10i).

Notes: *Navicula* cf. *consentanea* is a motile form, which colonized *Eudendrium racemosum* year round with quite high densities. The annual peak occurred in winter. It was distributed in all parts of the *E. racemosum* colony with preference for the central and apical parts.

Remarks on taxonomy: Specimens described in the literature (see references above) agree with our specimens, except for the valve shape, which is slightly more narrow in our samples. Therefore, "cf." has been added in the text to support these differences.

Surirellales

Surirellaceae

Campylodiscus C.G.Ehrenberg ex F.T.Kützing

Campylodiscus cf. ***clevei*** Leuduger-Fortmorel (1892) (Figures 11a–11c)

Refs: Leuduger-Fortmorel, 1892; Peragallo and Peragallo, 1897–1908.

Meas.: Diameter: 29–33 µm; TS in 10 µm: 3–4.

Description: Cell isopolar, saddle-shaped (Figures 11a and 11c), usually lying in valve view (Figure 11a). Valves subcircular with frustule bent in girdle view, convex along the apical plane, concave along the transapical plane (Figures 11a and 11c). Raphe submarginal, running around the whole perimeter of the valve and opening inwardly into a tubular canal raised on a ridge (Figure 11b). The canal raphe is separated from the remainder of the cell interior by fibulae (Figures 11a and 11b). Axial area lanceolate (Figure 11a, white arrow), from which depart robust ribs terminating close to the valve margin, with pyriform cups (Figures 11b, arrow; 11c). Striae multiseriate, consisting of small circular areolae occluded by hymens (Figure 11b). Two raphe endings in each hemivalve similar in shape (Figure 11a, black arrow).

Notes: *Campylodiscus* cf. *clevei* is a motile form. It is occasionally present on the colony of *Eudendrium racemosum* with higher density in spring and early summer. It is distributed in every colony part.

Remarks on taxonomy: Specimens described in the literature (see references above) agree with our specimens, except for the diameter of the valve, which is higher than in our samples (i.e. 75–90 µm in Peragallo and Peragallo, 1897–1908). Therefore, "cf." has been added in the text to support these differences.

Campylodiscus cf. ***decorus*** Brébisson (1854) (Figures 11d–11f)

Refs: Brébisson, 1854; Peragallo and Peragallo, 1897–1908; Witkowski et al., 2000; Lobban et al., 2012.

Meas.: Diameter: 23–25 µm; striae in 10 µm: 4.

Description: Cell isopolar, saddle-shaped (Figure 11d), usually lying in valve view (Figure 11d). Valves subcircular, appearing elliptical with the frustules bent in girdle view (Figure 11d). Raphe submarginal, running around the whole perimeter of the valve and opening inwardly into a tubular canal raised on a ridge (Figure 11d). Axial area lanceolate and narrow (Figure 11d, arrow). The pyriform cups occur on the valve margin (Figures 11d–11f, arrow). Striae multiseriate, consisting of small circular areolae (Figures 11e and 11f).

Notes: *Campylodiscus* cf. *decorus* is a motile form. It occurred rarely on the colony of *Eudendrium racemosum* with higher density in spring and early summer, without a marked spatial gradient along the colony.

Remarks on taxonomy: Specimens described in the literature (see references above) agree with our specimens, except for the diameter of the valve, which is higher than in our samples (i.e. 80–170 µm in Peragallo and Peragallo, 1897–1908; 35–105 µm in Witkowski et al., 2000). Moreover, Witkowski et al. (2000) showed a wide lanceolate sternum compared to the sternum that occurs in our samples. Therefore, "cf." has been added in the text to support these differences.

Campylodiscus decorus* var. *pinnatus H.Peragallo (1888) (Figures 11g–11h)

Refs: Peragallo, 1888; Peragallo and Peragallo, 1897–1908 (as var. *pinnata*); Ricard, 1987; Lobban et al., 2012.

Meas.: Diameter: 23–24 µm; striae in 10 µm: 4.

Description: var. *pinnatus* differs from the nominal variety in the irregularly placed, small spines that adorn the ribs (Figures 11g–11h).

Notes: *Campylodiscus decorus* var. *pinnatus* is a motile form. It occurred rarely on the colony of *Eudendrium racemosum* with higher density in spring and early summer, without a marked spatial gradient along the colony.

Campylodiscus cf. ***fastuosus*** Ehrenberg (1845) (Figures 12a and 12b)

Refs: Ehrenberg, 1845; Poulin et al., 1987; Paddock, 1985.

Meas.: Diameter: 11–33 µm; striae in 10 µm: 3–4.

Description: Cell isopolar, usually lying in valve view (Figure 12a). Frustules are bent in girdle view, each valve being saddle-shaped (Figure 12a). Raphe submarginal, running around the whole perimeter of the valve and opening inwardly into a tubular canal raised on a ridge or keel (Figures 12a and 12b). The canal raphe is separated from the remainder of the cell interior by fibulae (Figure 12b). Axial area linear (Figure 12a, arrow), from which depart ribs terminating in hyaline area from each side of the valve (Figures 12a; 12b, black arrow); from every hyaline area, branches of the large ribs (3–6 in 10 µm) end close to the valve margin, with pyriform cups (Figure 12b, white arrow). Striae bi/triseriate close to the axial areas and multiseriate in the rest of the valve, consisting of small circular areolae (Figure 12b).

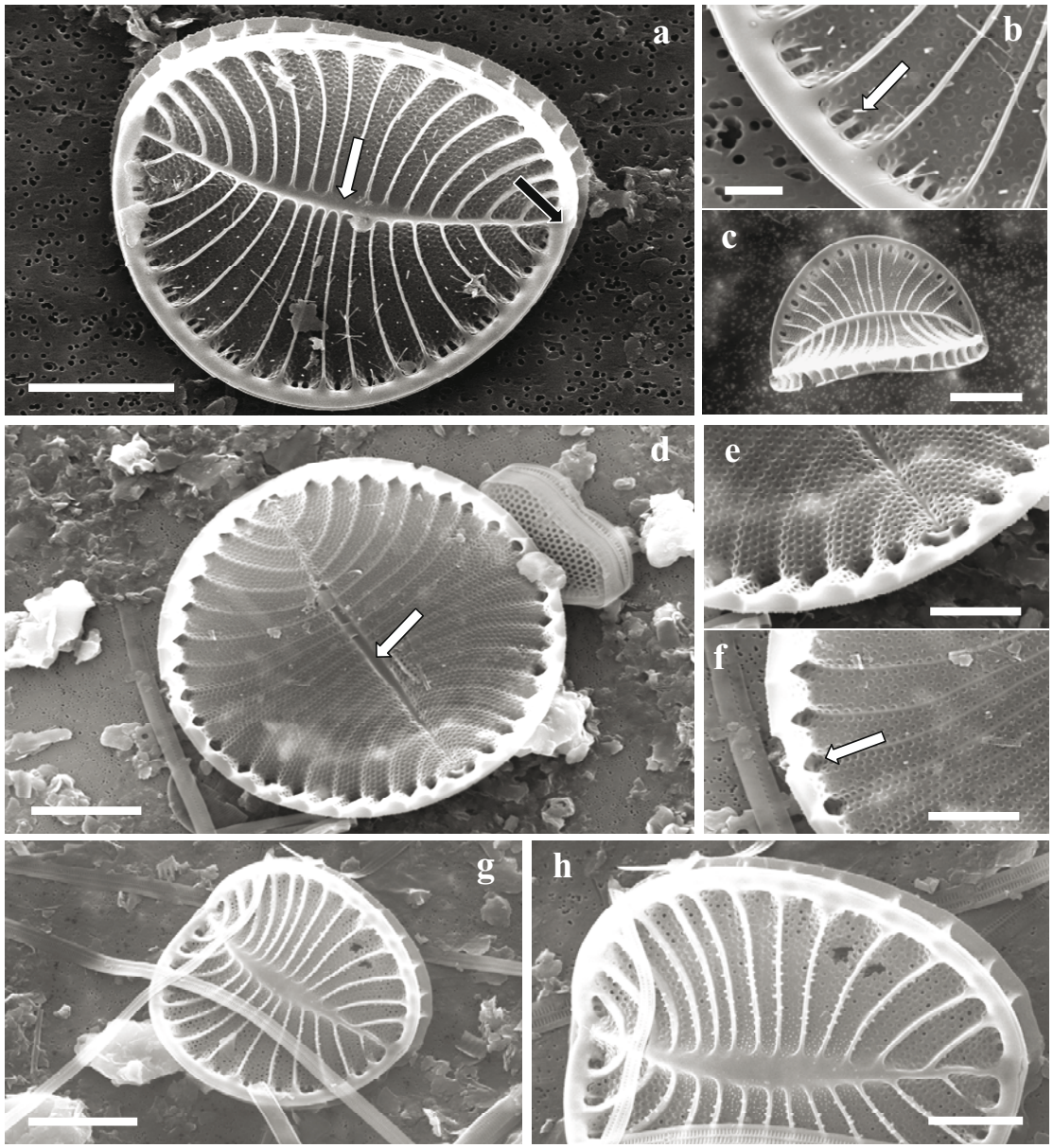

Figure 11. a–c= *Campylodiscus* cf. *clevei*, SEM. **a=** Internal valve face showing axial area (white arrow) and raphe endings (black arrow). **b=** Raphe with fibulae, pyriform cups (arrow), and multiseriate striae. **c=** Cell in girdle view, where the bending is clearly visible. **d–f=** *Campylodiscus* cf. *decorus*, SEM. **d=** External valve view showing axial area (arrow) and areolae. **e=** Apical region of the valve with ribs terminating close to the margin. **f=** Areolae on the valve face and pyriform cups (arrow). **g–h=** *Campylodiscus decorus* var. *pinnata*, SEM. **g=** Internal valve. **h=** Valve face with rounded areolae and small spines that adorn the ribs. Scale bars: a, c, d, g = 10 µm; e, f, h = 5 µm; b = 2 µm.

Notes: *Campylodiscus* cf. *fastuosus* is a motile form. As all the other *Campylodiscus* spp., it occurred only occasionally on the colony of *Eudendrium racemosum* with higher density in spring and early summer. It was distributed in every colony part.

Remarks on taxonomy: Specimens described in the literature (see references above) agree with our specimens, except for the diameter of the valve, which is higher than in our samples (e.g., 50–81 µm long, 54–79 µm wide in Poulin et al., 1987). Therefore, "cf." has been added in the text to support these differences.

Surirella scalaris Giffen (Witkowski et al., 2000; Hein et al., 2008; Lobban et al., 2012), appears to be similar, but is smaller and rather spinier than our specimens. Indeed, our samples of *C.* cf. *fastuosus* lack of the spines on its surface. Moreover, our valves show a higher number of

the ribs than *S. scalaris*. Finally, valves in *Surirella scalaris* are orientated in parallel while in *Campylodiscus* they are oriented at right angles to one another (Lobban et al., 2012).

Campylodiscus cf. ***thuretii*** Brébisson (1854) (Figures 12c–12g)

Refs: Brébisson, 1854; Van Heurck, 1880–1885; Shim, 1977.

Meas.: Diameter: 14–30 µm; striae in 10 µm: 3–4.

Description: Cell isopolar, typically lying in valve view (Figure 12c). Frustules are curved in girdle view, each valve being saddle-shaped (Figures 12c and 12d). Raphe submarginal, running around the whole perimeter of the valve and opening inwardly into a tubular canal raised on a ridge. The canal raphe is separated from the remainder of the cell interior by very thick fibulae (Figures 12d, 12g, arrows). Axial area linear (Figures 12c, arrow; 12d), from which depart ribs terminating on hyaline area from each side of the valve (Figures 12c, 12d, arrows); from every hyaline area, branches of the very large ribs (4–5 in 10 µm) end close to the valve margin, with pyriform cups (Figure 12g). Striae bi/triseriate close to the axial areas and multiseriate in the rest of the valve, consisting of small circular areolae (Figures 12e–12g).

Notes: *Campylodiscus* cf. *thuretii* is a motile form and occurs on the colony of *Eudendrium racemosum* with higher density in spring and early summer. It is distributed in every colony part.

Remarks on taxonomy: Specimens described in the literature (see references above) agree with our specimens, except for the number of the rows of the ribs between the axial and hyaline area. The number of rows is higher in the specimens described in the literature (Van Heurck, 1880–1885) than in ours. Therefore, "cf." has been added in the text to support these differences. Moreover, *Campylodiscus thuretii* can be compared to *Surirella fastuosa* for its valve shape, but they have different structures on the valve surfaces (Van Heurck, 1880–1885; Lobban et al., 2012).

Surirellales

Surirellaceae

Surirella Turpin

Surirella ovata Kützing (1844) (Figures 12h and 12i)

Refs: Kützing, 1844; Van Heurck, 1880–1885; Peragallo and Peragallo, 1897–1908; Helmcke and Krieger, 1953; Gerloff and Natour, 1982; Granetti, 1984; Parra et al., 1984; Roemer et al., 1984; Rosowski et al., 1986; Poulin et al., 1987.

Meas.: AA: 25–28 µm; TA: 9–11 µm; striae in 10 µm: 31–32; infundibula in 10 µm: 7.

Description: Cells heteropolar, ovoid in valve view (Figures 12h and 12i). In valve view, concave with undulations parallel to the apical axis and bluntly rounded apices; mantle highly reduced (Figure 12h). Internally, infundibula and siliceous ridges irregularly spaced (Figure 12i). Externally, transapical striae radially toward the apexes (Figure 12h). Internally, very small round areolae (Figure 12i). Raphe system runs around the valve perimeter, subtended internally by fibulae (Figures 12g and 12h).

Notes: *Surirella ovata* is a motile form that occurred with low densities on the *Eudendrium racemosum* colony, only from autumn to winter.

3.3. Monoraphid diatoms

Achnanthales

Achnanthaceae

Achnanthes Bory de Saint-Vincent

Achnanthes brevipes C.Agardh (1824) (Figures 13a–13g)

Refs: C.Agardh, 1824; Van Heurck, 1880–1885; Peragallo and Peragallo, 1897–1908; Helmcke and Krieger, 1953; Desikachary, 1957; Okuno, 1970; Alfinito, 1983; Ehrlich and Dor, 1985; Ricard, 1987.

Meas.: AA: 23–80 µm; TA: 10–26 µm; SV striae in 10 µm: 5–14; RSV striae in 10 µm: 5–14.

Description: Cells heterovalvar, linear-elliptical, bent along the median transapical plane (Figure 13d) with a concave raphe valve (Figure 13b) and a convex araphid valve (Figure 13a). Rapheless valve showing a narrow sternum lacking a central area and several robust transapical ribs, radial near the apices (Figures 13a and 13g). Raphid valve with an almost straight raphe, which terminated in slightly expanded pores on the center (Figure 13f); distal terminal fissures hooked (Figure 13e). Raphe-sternum is dilated in the center, forming a transapical hyaline fascia up to the margin (Figures 13e and 13f). Internally, the almost straight raphe is bordered by ribs; valve face shows a fascia and transapical ribs (Figure 13c). Striae are uni- or biseriate and consist of areolae occluded by complex cribra bearing volae (Figure 13g). Girdle consists of several open bands, which sometimes have wavy edges (Figure 13d). Rows of areolae are present on bands occluded by volae (Figure 13d).

Notes: *Achnanthes brevipes* attaches to the substrata with gelatinous stalk secreted from the raphe, having a variable length. In colonies, only the cell directly attached to the substratum produces the gelatinous peduncle, while the other cells attach to each other through the valve face. It occurred from autumn to spring in the central and upper part of the *Eudendrium racemosum* colony.

Achnanthes longipes C.Agardh (1824) (Figures 14a–14g)

Refs: Agardh, 1824; Van Heurck, 1880–1885; Peragallo and Peragallo, 1897–1908; Okuno, 1953; Hendey, 1959; Okuno, 1959; Geissler et al., 1961; Hendey, 1964; Drum et al., 1966; Hasle, 1973; Ohgai et al., 1984; Booth, 1987; Daniel et al., 1987; Round et al., 1990.

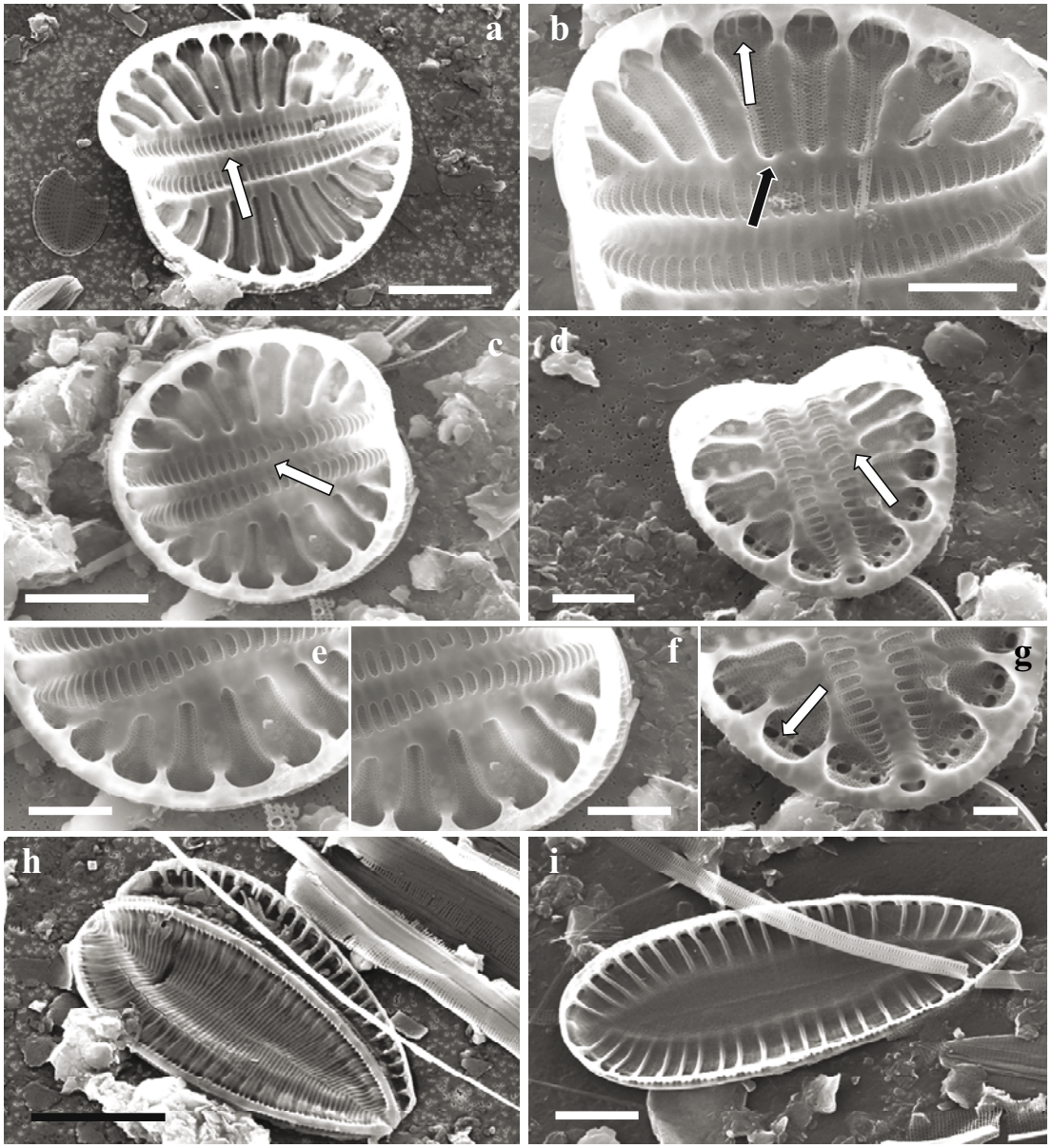

Figure 12. a–b= *Campylodiscus* cf. *fastuosus*, SEM. **a.** Internal valve view. **b**= Part of valve showing pyriform cups (white arrow) on the margin and hyaline area (black arrow). **c–g**= *Campylodiscus* cf. *thuretii*, SEM. **c**= Internal valve view showing axial area (arrow). **d**= Internal valve face showing the bent frustule and hyaline area (arrow). **e**= Multiseriate striae. **f**= Multiseriate and biseriate striae. **g**= Apical region of the valve with ribs terminating with pyriform cups and fibulae (arrow) in the canal raphe. **h–i**= *Surirella ovata*, SEM. **h**= External valve view. **i**= Internal valve view with infundibula. Scale bars: a, c, h = 10 µm; b, d–f, i = 5 µm; g = 2 µm.

Meas.: AA: 37–110 µm; TA: 8–20 µm; SV striae in 10 µm: 4–8; RSV striae in 10 µm: 5–6.

Description: Cells heterovalvar, almost elliptical, bent along the median transapical plane (Figures 14a, 14b, and 14d) with a concave raphid valve (Figure 14c) and a convex rapheless valve (Figure 14a). Rapheless valve showing both internally and externally a narrow sternum lacking a central area and several transapical ribs, slightly radial near the apices (Figures 14a and 14b). Raphid valve showing externally an almost straight raphe, which terminated in simple pores at the center (Figure 14e); distal terminal fissures bent (Figure 14f). Raphe-sternum is dilated in the center, forming a transapical hyaline fascia up to the margin (Figures 14c and 14e). Striae are biseriate and triseriate and consist of areolae occluded by cribra both on raphid valve and on rapheless valve (Figures

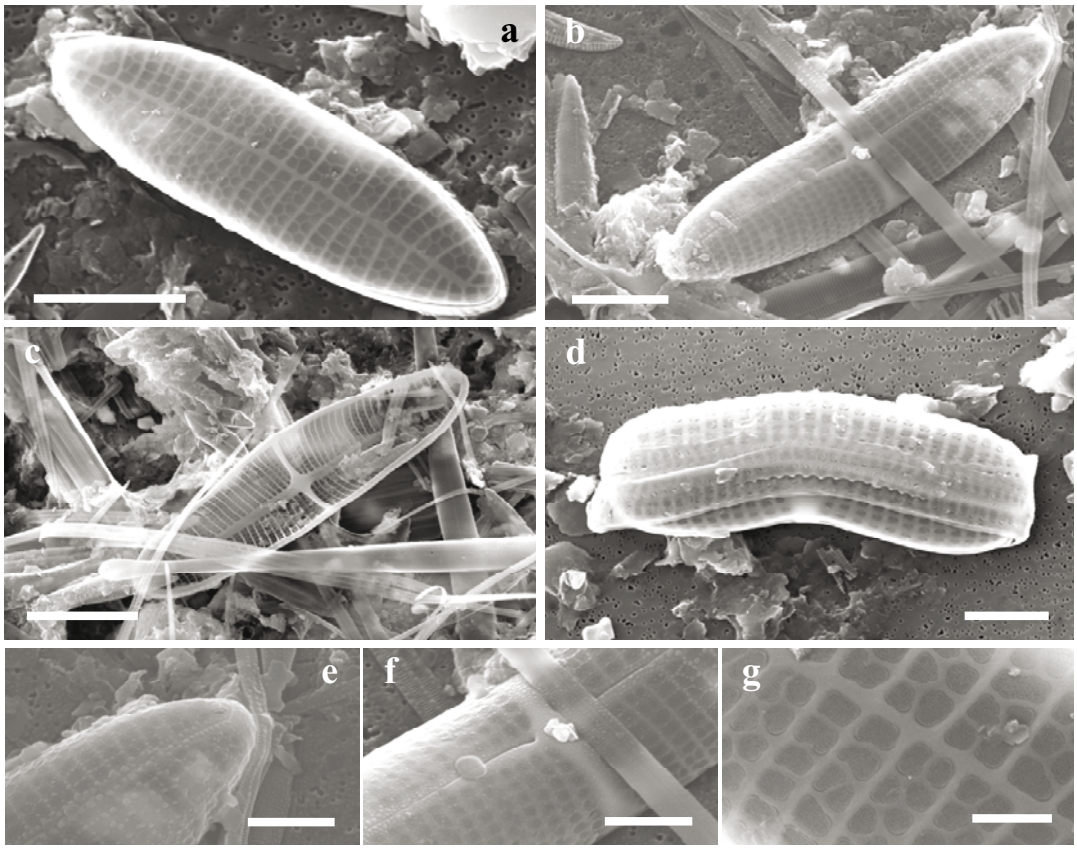

Figure 13. a–g= *Achnanthes brevipes*, SEM. **a**= External valve view of the rapheless valve. **b**= External valve view of a raphid valve. **c**= Internal valve view of a raphid valve with transapical ribs. **d**= Girdle view bent formed by several open bands. **e**= Apical region of the valve showing hooked terminal raphe fissure. **f**= External central raphe endings and hyaline fascia. **g**= Uni- and biseriate striae on the external rapheless valve. Scale bars: c = 20 µm; a, b = 10 µm; d–f = 5 µm; g= 2 µm.

14a–14g). Girdle consists of several bands with punctuate striae parallel to the pervalvar axis (Figure 14d).

Notes: *Achnanthes longipes* attaches to the substrata with gelatinous stalk secreted from the raphe, having a variable length. In colonies, only the cell directly attached to the substratum produces the gelatinous peduncle, while the other cells attach to each other through the valve face. It occurred from autumn to spring in the central and upper part of the *Eudendrium racemosum* colony.

4. Discussion

Epizoic diatoms are important components of benthic communities, both of marine and freshwater areas (Totti et al., 2011). Nevertheless, the knowledge of their biodiversity and spatiotemporal distribution trends has long been neglected, especially in marine environments.

The marine hydroid *Eudendrium racemosum* hosts a complex and diversified community of epibenthic microalgae (Romagnoli et al., 2007), with marked seasonal variability and with abundances significantly higher than those reported for other epizoic communities (Bodeanu, 1987–1988; Gillan and Cadée, 2000; Patil and Anil, 2000). Epibenthic diatoms seem to gain advantages from their living hosts, as suggested by the significantly higher densities found on hydroid than on mimic plastic substrata (Romagnoli et al., 2007). The advantages for microalgae in colonizing animals are related to several aspects: the host's catabolites (both nutrients and CO_2) markedly enhance the microalgal growth (Totti et al., 2011), and microalgae benefit from a raised position with better light exposure and obtain protection against grazing, which is more effective if the animal host is motile (Totti et al., 2005, 2011). Moreover, hosts simply offer additional substrata to be colonized by benthic diatoms (Round, 1981; Totti et al., 2011).

In this study, we reported the SEM descriptions of the most representative epizoic diatoms associated with *Eudendrium racemosum*, with attention to their growth forms. Among motile diatoms, the most significant for biodiversity were *Navicula* cf. *consentanea*, *Caloneis*

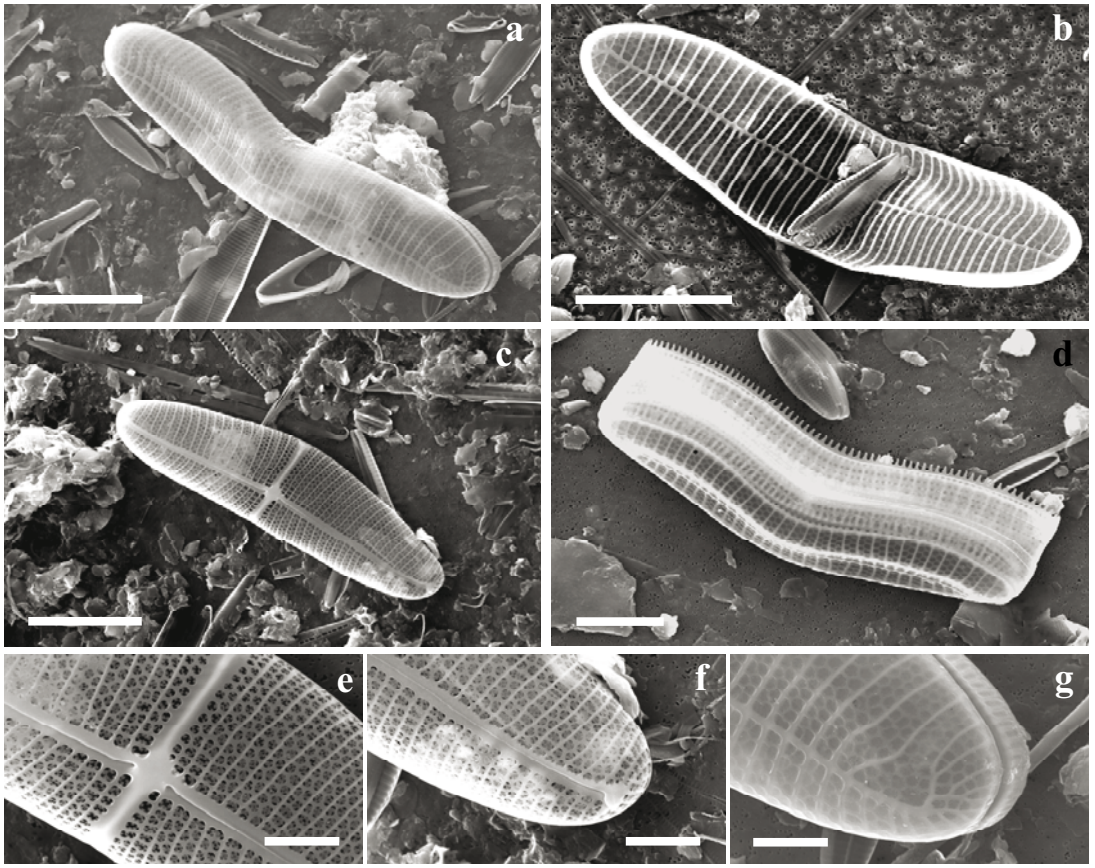

Figure 14. a–g= *Achnanthes longipes*, SEM. **a=** External valve view of rapheless valve. **b=** Internal valve view of rapheless valve with a sternum and transapical ribs. **c=** Valve view of a raphid valve. **d=** Girdle view of the valve. **e=** Central area with terminal simple pores of the raphe and a transapical hyaline fascia. **f=** Apical area with bent terminal raphe fissure. **g=** Apical area of rapheless valve with biseriate striae. Scale bars: a–c = 20 µm; d = 10 µm; e–g = 5 µm.

alpestris, *Psammodictyon mediterraneum*, *Diploneis oculata*, and *Tryblionella marginulata* var. *subconstricta* f. *minuta*. On average, motile diatoms represented the most abundant fraction of diatom communities, and they showed a maximum abundance in winter and minimum in summer (Romagnoli et al., 2007). Motile forms are considered to be highly favored due to their ability to move into mature mats, making them superior competitors for nutrients and light (DeNicola and McIntire, 1990). The most important adnate taxa observed on *Eudendrium racemosum* belong to the genera *Cocconeis* and *Amphora*. Adnate diatoms showed 2 peaks in autumn-winter and in spring-early summer, while a decrease was observed in late winter. Due to their adhering mode on the host surface through the valve face, adnate taxa may easily benefit from the nutrient exchange with the host (Round, 1981; Sullivan, 1984) and their temporal trend reflected the annual cycle of hydroid host (Romagnoli et al., 2007). Erect diatoms were represented mainly by *Licmophora* spp., *Grammatophora* spp., *Tabularia tabulata*, and *Cyclophora tenuis*; they had their annual maximum between autumn and spring, with a marked decrease in summer. Erect diatoms have better access to light, although they are more exposed to grazing pressures (Müller, 1999; Hillebrand et al., 2000), and their capability of regulating stalk lengths makes them competitors for light when dense benthic populations develop. Their decrease in summer may be related either to the effect of exceptionally high temperatures recorded during summer 2003 or to an effect of increased grazing pressure. Moreover, tube-dwelling species (mainly *Berkeleya rutilans*) were also recorded, with maximum values in summer, although no significant differences were recorded among seasons. In general, diatom abundances were significantly higher in the apical part of the hydroid colony, whereas only adnate diatoms were more abundant in the basal and central parts.

A comparison with the diatom flora associated with other invertebrates is not easy, as (i) different host

species are involved, (ii) different areas are considered, and (iii) not all other studies reported the list of taxa. Comparing the list of species found on *Eudendrium racemosum* with other species lists from other studies on epiphytic (seaweeds, seagrasses, mangroves), epilithic (natural and artificial hard substrata), and epizoic (marine invertebrates) diatoms, the more common species on all substrata were *Cocconeis scutellum* with its varieties and *C. molesta* var. *crucifera*, followed by *Grammatophora marina* and *Amphora coffeaeformis* (Round et al., 1961; Sullivan, 1975, 1978, 1979, 1980; Korte and Blinn, 1983; Sullivan, 1984; Siqueiros-Beltrones et al., 1985; Tanaka, 1986; Moncreiff et al., 1992; Carman and Dobbs, 1997; Wuchter et al., 2003; Siqueiros-Beltrones et al., 2005a, 2005b; Totti et al., 2007, 2009; Chen et al., 2010), which seem to be the most ubiquitous and do not seem to have preference for either the geographic region or for the type of substrate. Through this study, some of these species, such as *Diatoma anceps*, *Licmophora reichardtii*, *Licmophora* cf. *dalmatica*, *Caloneis alpestris*, *Navicula* cf. *consentanea*, *Campylodiscus* cf. *clevei*, *Campylodiscus* cf. *decorus* (from the Protist Central website there is uncertain identification: http://www.protistcentral.org/Project/get/project_id/17) and *Campylodiscus* cf. *thuretii*, were described for the first time through SEM analysis.

In conclusion, the taxonomic knowledge and the morphological data of the species observed in the present study were improved and updated. Moreover, additional information about biodiversity of the Mediterranean Sea was given.

Acknowledgments

The authors gratefully acknowledge Giorgio Bavestrello for collecting hydroid samples. Special thanks are given to the anonymous reviewers, who contributed to improving this work.

References

Agardh CA (1824). Systema Algarum. Lund: Literis Berlingianis.

Agardh CA (1827). Aufzählung einiger in den österreichischen Ländern gefundenen neuen Gattungen un Arten von Algen nebst Diagnostik und beigefügten Bemerkungen. Flora oder Botanische Zeitung 10: 625–645.

Agardh CA (1831). Conspectus Criticus Diatomacearum. Part 3. Lund: Literis Berlingianis.

Agardh CA (1832). Conspectus Criticus Diatomacearum. Part 4. Lund: Literis Berlingianis.

Akbulut A (2003). Planktonic Diatom (Bacillariophyceae) flora of Sultan Sazlığı marshes (Kayseri). Turk J Bot 27: 285–301.

Alfinito S (1983). The phytoplankton of the Lake of Bracciano (Latium, Italy) during 1977–1978. Preliminary observations. Annali di Botanica, Roma 41: 77–79.

Anderson OR (1975). The ultrastructure and cytochemistry of resting cell formation in *Amphora coffaeformis* (Bacillariophyceae). J Phycol 11: 272–281.

Archibald REM (1983). The diatoms of the Sundays and Great Fish Rivers in the eastern Cape Province of South Africa. Bibliotheca Diatomologica 1: 1–362.

Archibald REM, Barlow DJ (1983). On the raphe ledge in the genus *Amphora* (Bacillariophyta). Bacillaria 6: 257–266.

Archibald REM, Schoeman FR (1984). *Amphora coffeaeformis* (Agardh) Kützing: a revision of the species under light and electron microscopy. S Afr J Bot 3: 83–102.

Bavestrello G, Cerrano C, Di Camillo C, Puce S, Romagnoli T, Tazioli S, Totti C (2008). The ecology of protists epibiontic on marine hydroids. J Mar Biol Assoc Uk 88: 1611–1617.

Begin ZB, Ehrlich A, Nathan Y (1974). Lake Lisan, the Pleistocene precursor of the Dead Sea. Jerusalem: Geological Survey of Israel Bulletin 63.

Beihette Symposium (1975). Proposal for a standardization of diatom terminology and diagnoses. Nova Hedwigia 53: 323–354.

Bennett AG (1920). On the occurrence of diatoms on the skin of whales with an Appendix by EW Nelson. Royal Society of London Proceedings 91: 352–357.

Bérard-Therriault L, Cardinal A, Poulin M (1986). Les diatomées (Bacillariophyceae) benthiques de substrats durs des eaux marines et saumâtres du Québec. 6. Naviculales: Cymbellaceae et Gomphonemaceae. Le Naturaliste Canadien 113: 405–429.

Bodeanu N (1987–1988). Structure et dynamique de l'algoflore unicellulaire dans les eaux du littoral romain de la mer Noire. Recherches Marines IRCM 20: 19–250.

Booth WE (1987). Contribution by diatoms to marine algal host-epiphyte photosynthesis. Bot Mar 30: 129–140.

Bory de Saint-Vincent JBM (1831). Dictionnaire Classique d'Histoire Naturelle. Atlas et illustration des planches. Vol. 17. Paris: Libraires-Éditeurs.

Boyer CS (1926–1927). Synopsis of the North American Diatomaceae. Part II. P Acad Nat Sci Phila 79: 229–583.

Bradbury JP, Blair WN (1979). Paleoecology of the upper Miocene Hualapai Limestone Member of the Muddy Creek Formation, Northwestern Arizona. In: RMAG-UGA Basin and Range Symposium, pp. 293–303.

Cardinal A, Poulin M, Bérard-Therriault L (1984). Les diatomées benthiques de substrats durs des eaux marines et saumâtres du Québec. 4. Naviculales, Naviculaceae (à l'exclusion des genres *Navicula*, *Donkinia*, *Gyrosigma* et *Pleurosigma*). Le Naturaliste Canadien 111: 369–394.

Carman KR, Dobbs FC (1997). Epibiotic microorganisms on copepods and other marine crustaceans. Microsc Res Techniq 37: 116–135.

Castracane F (1878). Nuovo genere e specie di Diatomea. Atti dell'Accademia Pontificia de'Nuovi Lincei 31: 1–11.

Cerrano C, Calcinai B, Cucchiari E, Di Camillo C, Nigro M, Regoli F, Sarà A, Schiaparelli S, Totti C, Bavestrello G (2004). Are diatoms a food source for Antarctic sponges? Chem Ecol 20: 57–64.

Cerrano C, Calcinai B, Cucchiari E, Di Camillo C, Totti C, Bavestrello G (2004b). The diversity of relationships between Antarctic sponges and diatoms: the case of *Mycale acerata* Kirkpatrick, 1907. Polar Biol 27: 231–337.

Chen CP, Gao YH, Lin P (2010). Geographical and seasonal patterns of epiphytic diatoms on a subtropical mangrove (*Kandelia candel*) in southern China. Ecol Indic 10: 143–147.

Cleve PT (1885). On some fossil marine diatoms found in the Moravian "Tagel" from Augarten, near Brünn. Journal of the Quekett Microscopical Club 2: 165–177.

Cleve PT (1894). Synopsis of the Naviculoid Diatoms, Part I. Kongliga Svenska-Vetenskaps Akademiens Handlingar 26: 1–194.

Cleve PT, Grunow A (1880). Beiträge zur Kenntniss der Arctischen Diatomeen. Kongliga Svenska-Vetenskaps Akademiens Handlingar 17: 1–121.

Çolak Sabancı F (2012). An illustrated survey on the morphological characters in three species of the diatom genus *Mastogloia* (Bacillariophyceae). Turk J Bot 36: 727–737.

Çolak Sabancı F, Koray T (2010). Four new records for the benthic diatoms (genera *Cocconeis*, *Seminavis*, *Synedra*, and *Trachysphenia*) from the Aegean Sea. Turk J Bot 34: 531–540.

Compère P (1981). Algues des désertes d'Iran. Bulletin du Jardin Botanique National de Belgique 51: 3–40.

Compère P, Delmotte A (1988). Diatoms in two hot springs in Zambia (Central Africa). In: Proceedings of the 9th International Diatom Symposium, pp. 29–39.

Cooksey KE, Cooksey B (1986). Adhesion of fouling diatoms to surfaces: some biochemistry. In: Evans LV, Hoagland KD, editors. Algal Biofouling. New York: Elsevier, pp. 41–53.

Cox EJ (1977). Raphe structure of naviculoid diatoms as revealed by the scanning electron microscope. Nova Hedwigia 54: 261–274.

Cox EJ (1981). Mucilage tube morphology of three tube-dwelling diatoms and its diagnostic value. J Phycol 17: 72–80.

Cupp EE (1943). Marine Plankton Diatoms of the West Coast of North America. Berkeley: University of California Press.

D'Alelio D, Cante M, Russo GF, Totti C, De Stefano M (2011). Epizoic diatoms on gastropod shells: when substrate complexity selects for microcommunity complexity. In: Seckbach J, Dubinsky Z, editors. All Flesh is Grass: Plant-Animal Interrelationships, Vol. 16. Cellular Origin and Life in Extreme Habitats and Astrobiology. Dordrecht: Springer, pp. 1–532.

Daniel GF, Chamberlain AHL, Jones EBG (1987). Cytochemical and electron microscopical observations on the adhesive materials of marine fouling diatoms. Brit Phycol J 22: 101–118.

DeNicola DM, McIntire CD (1990). Effects of substrate relief on the distribution of periphyton in laboratory streams. I. Hydrology. J Phycol 26: 624–633.

Desikachary TV (1957). Electron microscope studies on diatoms. Journal of the Royal Microscopical Society 76: 9–36.

Desmazières JBHT (1854). Plantes cryptogames de la France. Lille: Taylor and Francis Group.

De Stefano M, Marino D, Mazzella L (2000). Marine taxa of *Cocconeis* on leaves of *Posidonia oceanica*, including a new species and two new varieties. Eur J Phycol 35: 225–242.

De Stefano M, Romero O (2005). A survey of alveolate species of the diatom genus *Cocconeis* (Ehr.) with remarks on the new section Alveolatae. Bibliotheca Diatomologica 52: 1–132.

De Stefano M, Romero OE, Totti C (2008). A comparative study of *Cocconeis scutellum* Ehrenberg and its varieties (Bacillariophyta). Bot Mar 51: 506–536.

De Toni JB (1892). Sylloge algarum omnium hucusque cognitarum. Vol. 2. Bacillarieae. Sectio 2, Pseudhoraphidee. Typis seminarii. Padua: Sumptibus Auctoris.

Di Camillo C, Puce S, Romagnoli T, Tazioli S, Totti C, Bavestrello G (2005). Relationships between benthic diatoms and hydrozoans (Cnidaria). J Mar Biol Assoc UK 85: 1373–1380.

Dor I, Ehrlich A (1987). The effect of salinity and temperature gradients on the distribution of littoral microalgae in experimental solar ponds, Dead Sea area, Israel. Mar Ecol 8: 193–205.

Drum RW, Pankratz HS, Stoermer EF (1966). Electron microscopy of diatom cells. In: Helmcke JG, Krieger W, editors. Diatomeenschalen im elektronenkroskopischen Bild. Vol. 6. Lehre: Cramer, pp. 514–613.

Ehrenberg CG (1832). Beiträge zur Kenntnifs der Organisation der Infusorien und ihrer geographischen Verbreitung, besonders in Sibirien. Abhandlungen der Königlichen Akademie der Wissenschaften zu Berlin 1830: 1–88.

Ehrenberg CG (1838). Die Infusionsthierchen als vollkommende Organismen. Ein Blick in das tiefere organische Leben der Natur. Leipzig: Leopold Voss.

Ehrenberg CG (1840). Über noch zahlreich jetzt lebende Thierarten der Kreidebildung und den Organismus der Polythalamien. Leipzig: Leopold Voss.

Ehrenberg CG (1843). Verbreitung und Einfluss des mikroskopischen Lebens in Süd-und Nord-Amerika. Abhandlungen der Königlichen Akademie der Wissenschaften zu Berlin 1841: 291–466.

Ehrenberg CG (1845). Novorum Generum et Specierum brevis definitio. Zusätze zu seinen letzten Mittheilung über die mikroskopischen Lebensformen von Portugall und Spanien, Süd-Afrika, Hinter-Indien, Japan und Kurdistan, und legte die folgenden Diagnosen. Bericht über die zur Bekanntmachung geeigneten Verhandlungen der Königlich-Preussischen Akademie der Wissenschaften zu Berlin 1845: 357–377.

Ehrlich A (1978). The diatoms of the hyperhaline Solar Lake (NE Sinai). Israel J Bot 27: 1–13.

Ehrlich A, Dor I (1985). Photosynthetic microorganisms of the Gavish Sabkha. Hypersaline Ecosystems 53: 296–321.

Gasse F (1971). Organisation ultrastructurale de colonies de quelques diatomées penées araphidées, révelée par le microscope électronique à balayage. Comptes rendus de l'Académie des Sciences D 272: 3169–3172.

Geissler U, Gerloff J, Helmcke JG, Krieger W, Reimann B (1961). Diatomeenschalen im elektronenmikroskopischen Bild. Vol. 3. Weinheim: J Cramer, pp. 201–300.

Geissler U, Gerloff J, Helmcke JG, Krieger W, Reimann B (1963). Diatomeenschalen im elektronenmikroskopischen Bild. Vol. 4. Weinheim: J Cramer, pp. 301–413.

Gerloff J, Natour RM (1982). Diatoms from Jordan. II. Beih. Nova Hedwigia 73: 157–209.

Germain H (1979). Details of structure in three small freshwater *Diploneis*. Nova Hedwigia 64: 207–217.

Germain H (1981). Flore des diatomées (Diatomophycées) eaux douces et saumâtres du Massif Armoricain et des contrées voisines d'Europe occidentale. Collection Faunes et Flores actuelles. Paris: Editions Boubée.

Gillan DC, Cadée GC (2000). Iron-encrusted diatoms and bacteria epibiotic on *Hydrobia ulvae* (Gastropoda: Prosobranchia). J Sea Res 43: 83–91.

Gleser SI, Makarova IV, Moiseeva AI, Nikolaev VA (1988). The Diatoms of the USSR. Fossil and Recent. Vol. 2. Fasc. 1. Pyxidiculaceae, Thalassiosiropsidaceae, Triceratiaceae, Thalassiosiraceae. Leningrad: Nauka.

Granetti B (1984). Le Diatomee del Lago Trasimeno: sistematica ed ecologia. Rivista di Idrobiologia 23: 1–112.

Gregory W (1857). On new forms of marine Diatomaceae found in the Firth of Clyde and in Losh Fyne. T Roy Soc Edin 21: 473–542.

Greville RK (1827). Scottish Cryptogamic Flora or Coloured Figures and Descriptions of Cryptogamic Plants Found in Scotland and Belonging Chiefly to the Order Fungi and Intended to Serve as a Continuation of English Botany. Vol. 5. Edinburgh: MacLachlan and Stewart.

Grunow A (1860). Ueber neue oder ungenügend gekannte Algen. Erste Folge, Diatomeen, Familie Naviculaceen. Verhandlungen der Kaiserlich-Königlichen Zoologisch-Botanischen Gesellschaft in Wien 10: 503–582.

Grunow A (1862). Die österreichischen Diatomaceen nebst Anschluss einiger neuen Arten von andern Lokalitäten und einer kritischen Uebersicht der bisher bekannten Gattungen und Arten. Erste Folge. Epithemieae, Meridioneae, Diatomeae, Entopyleae, Surirelleae, Amphipleureae. Zweite Folge. Familie Nitzschieae. Verhandlungen der Kaiserlich-Königlichen Zoologisch-Botanischen Gesellschaft in Wein 12: 315–472, 545–588.

Grunow A (1867). Reise seiner Majestät Fregatte Novara um die Erde. Botanischer Theil. Band I. Algen. Vienna: Kaiselich-Königlichen Hof-und Staasdruckerei.

Grunow A (1880). Vorlaufige Bemerkungen zu einer systematischen Anordung der *Schizonema- und Berkeleya*-Arten, mit Bezug auf die in Van Heurck's Diatomeenflora von Belgien veröffentlichten Abbildungen der Frusteln auf Taf. 15, 16 und 17. Part II. Botanisches Centralblatt 4: 1585–1598.

Guslyakov NE (1985). On the morphology of the frustules in some representatives genus *Amphora* (Bacillariophyta) from the Black Sea. Botanicheskij Zhurnal 70: 1478–1481.

Gusylakov NE (1988). New data on frustule morphology in the genus *Amphora* (Bacillariophyta). Botanicheskij Zhurnal 73: 342–349.

Hart TJ (1935). On the diatoms of the skin film of whales, and their possible bearing on problems of whale movements. Discovery Report 10: 247–282.

Hasle GR (1964). *Nitzschia* and *Fragilariopsis* species studied in the light and electron microscopes. I. Some marine species of the groups *Nitzschiella* and *Lanceolatae*. Skrifter Norske Videnskabers Akademie 16: 1–48.

Hasle GR (1973). The "mucilage pore" of pennate diatoms. Nova Hedwigia 45: 167–194.

Hasle GR, Syvertsen EE (1996). Marine diatoms. In: Tomas CR, editor. Identifying Marine Diatoms and Dinoflagellates. San Diego: Academic Press, pp. 5–385.

Hein MK, Winsborough BM, Sullivan MJ (2008). Bacillariophyta (diatoms) of the Bahamas. Iconographia Diatomologica 19. Ruggell: Gantner Verlag.

Heiberg PAC (1863). Conspectus criticus Diatomacearum Danicarum. Kritisk Oversigt over De Danske Diatomeer. Copenhagen: Wilhelm Priors Forlag.

Helmecke JG, Krieger W (1953). Diatomeenschalen in elektronenmikroskopischen Bild 1. Berlin: Transmare-Photo GMBH.

Helmecke JG, Krieger W (1954). Diatomeenschalen im elektronenmikroskopishen Bild 2. Berlin: Transmare-Photo GMBH.

Hendey NI (1959). The structure of the diatom cell wall as revealed by the electron microscope. Journal of the Quekett Microscopical Club 4: 147–175.

Hendey NI (1964). An Introductory Account of the Smaller Algae of British Coastal Waters. Part V. Bacillariophyceae (Diatoms). London: Her Majesty's Stationery Office.

Hillebrand H, Worm B, Lotze HK (2000). Marine microbenthic community structure regulated by nitrogen loading and grazing pressure. Mar Ecol-Prog Ser 204: 27–38.

Hiromi J, Takano H (1983). Preliminary note on pelagic marine copepods and their epizoic diatoms. Bulletin Plankton Society of Japan 30: 171–173.

Holmes RW (1985). The morphology of diatoms epizoic on cetaceans and their transfer from *Cocconeis* to two new genera, *Bennettella* and *Epipellis*. Brit Phycol J 20: 43–57.

Holmes RW, Crawford RM, Round FE (1982). Variability in the structure of the genus *Cocconeis* Ehr. (Bacillariophyta) with special reference to the cingulum. Phycologia 21: 370–381.

Honeywill C (1998). A study of British *Licmophora* species and a discussion of its morphological features. Diatom Res 13: 221–271.

Hudon C, Bourget E (1981). Initial colonization of artificial substrate: community development and structure studied by scanning electron microscopy. Can J Fish Aquat Sci 38: 1371–1384.

Hudon C, Legendre P (1987). The ecological implications of growth forms in epibenthic diatoms. J Phycol 23: 434–441.

Hustedt F (1930). Die Susswasserflora Mitteleuropas. Heft 10. 2nd ed. Bacillariophyta (Diatomeae). Jena: Verlag von Gustav Fischer.

Hustedt F (1933). Die Kieselalgen Deutschlands, Österreichs und der Schweiz unter Berücksichtigung der übrigen Länder Europas sowie der angrenzenden Meeresgebiete. In: Rabenhorst L, editor. Kryptogamen Flora von Deutschland, Österreich und der Schweiz, Vol 7. Leipzig: Akademische Verlagsgesellschaft, pp. 1–576.

Hustedt F (1939). Die Diatomeenflora des Küstengebietes der Nordsee vom Dollart bis zur Elbemündung. I. Die Diatomeenflora in den Sedimenten der unteren Ems sowie auf den Watten in der Leybucht, des Memmert und bei der Insel Juist. Abhandlungen des Naturwissenschaftlichen Verein zu Bremen 31: 571–677.

Husted F (1985). The Pennate Diatoms, A Translation of Hustedt's "*Die Kieselalgen*, 2 Teil", with supplement by N.H. Jensen. Koenigstein: Koeltz Scientific Books.

Idei M, Kobayasi H (1986). Observations on the valve structure of fresh water *Diploneis* (Bacillariophyceae), *D. oculata* (Brèb.) Cleve and *D. minuta* Petersen. Jpn J Phycol 34: 87–93.

Ikeda AT (1977). A pelagic marine copepod associated with diatoms. Bull Plankton Soc Jpn 24: 115–118.

Karayeva NI, Dzhafarova SK (1987). On the morphology of two pennate diatom species (Bacillariophyta). Botanicheskij Zhurnal 72: 1052–1057.

Karayeva NI, Dzhafarova SK (1988). Morphology of some polyhalobic diatoms in connection with changes in salinity. Botanicheskij Zhurnal 73: 477–485.

Karayeva NI, Gadzhieva MA (1975). Novitates ad cognitionem Bacillariophytorum e mari Caspico. I. Novosti Sistematiki Nizshikh Rastenii 12: 123–129.

Karayeva NI, Magerramova NR, Rhzaeva SG (1984). Morphology of the diatom frustule of the genus *Amphora* (Bacillariophyta) based on the data of electron microscopy. Botanicheskij Zhurnal 69: 492–497.

Kirchner O (1878). Algen. In: Cohn F, editor. Kryptogamen-Flora von Schlesien. Vol. 1. Breslau: Kern's Verlag, pp. 1–284.

Kooistra WHCF, De Stefano M, Mann DG, Salma N, Medlin LK (2003). Phylogenetic position of *Toxarium*, a pennate-like lineage within centric diatoms (Bacillariophyceae). J Phycol 39: 185–197.

Korte VL, Blinn DW (1983). Diatom colonization on artificial substrata in pool and riffle zones studied by light and scanning electron microscopy. J Phycol 19: 332–341.

Kützing FT (1844). Die kieselschalignen Bacillarien oder Diatomeen. Nordhausen: W. Köhne.

Kützing FT (1849). Species algarum. Leipzig: F.A. Brockhaus.

Leuduger-Fortmorel G (1892). Diatomées de la Malaisie. Annales du Jardin Botanique de Buitenzorg 11: 1–60.

Lobban CS (1984). Marine tube-dwelling diatoms of eastern Canada: descriptions, checklist, and illustrated key. Can J Bot 62: 778–794.

Lobban CS, Pennesi C (2014). Two new *Mastogloia* species (Bacillariophyceae), *M. parlibellioides* and *M. lyra* , from coral reefs in Guam, Western Pacific. Bot Mar 5: 41–54.

Lobban CS, Schefter M, Ruck EC (2011). *Licmophora flucticulata* sp. nov. (Licmophoraceae, Bacillariophyceae), an unusual flabellate species from Guam and Palau. Phycologia 50: 11–22.

Luttenton MR, Rada RG (1986). Effects of disturbance on epiphytic community architecture. J Phycol 22: 320–326.

Lyngbye HC (1819). Tentamen Hydrophytologiae Danicae. Sectio V. Homalogonata. Copenhagen: Gyldendal.

MacIntyre HL, Geider RJ, Miller DC (1996). Microphytobenthos: the ecological role of the secret garden of unvegetated, shallow-water marine habitats. I. Distribution, abundance and primary production. Estuaries 19: 186–201.

Majewska R, Gambi MC, Totti CM, Pennesi C, De Stefano M (2013). Growth form analysis of epiphytic diatom communities of Terra Nova Bay (Ross Sea, Antarctica). Polar Biol 36: 73–86.

Makarova IV, Akhmetova NI (1986). De Bacillariophytis pro lacu Balchasch novis. III. Novosti Sistematiki Nizshikh Rastenii 23: 57–64.

Makarova IV, Guslyakov NE (1984). On the morphology of valves in some species of the genus *Licmophora* (Bacillariophyta) from the Black Sea. Botanicheskij Zhurnal 69: 870–872.

Marion A, Rincé Y, Robert JM (1986). Phytoplancton printanier en Baie de Bourgneuf, entre ocean et marais maritimes. Bulletin Société des Sciences Naturelles de l'Ouest de la France 8: 1–9.

Moncreiff CA, Sullivan MJ, Daehnick AE (1992). Primary production dynamics in seagrass beds of Mississippi Sound: the contributions of seagrass, epiphytic algae, sand microflora, and phytoplankton. Mar Ecol Prog Ser 87: 161–171.

Müller U (1999). The vertical zonation of adpressed diatoms and other epiphytic algae on *Phragmites australis*. Eur J Phycol 34: 487–496.

Navarro JN (1982a). Marine diatoms associated with mangrove prop roots in the Indian River, Florida, USA. Bibliotheca Phycologica 61: 1–151.

Navarro JN (1982b). A survey of the marine diatoms of Puerto Rico. IV. Suborder Araphidineae: Families Diatomaceae and Protoraphidaceae. Bot Mar 25: 247–263.

Nikolaev VA, Dmitrash ZH (1985). Diatomea in ice samples from eastern Antarctic. Vestnik Leningradskogo Universiteta Geology Geography 14: 90–93.

Ohgai M, Matsui T, Okuda T, Tsukahara H (1984). Fine structure of adhesive parts of diatoms (Bacillariophyceae) and their adhesive mechanism. Journal of the Shimonoseki University of Fisheries 33: 27–35.

Okuno H (1953). Electron microscopical study of the fine structure of diatom frustules. X. Bot Mag Tokyo 66: 5–8.

Okuno H (1959). Electron microscopical study on fine structure of diatom frustules. XVII. Stereoscopic observation. Bot Mag Tokyo 72: 61–67.

Okuno H (1970). Marine diatoms. In: Helmcke JG, Krrieger W, editors. Diatomeenschalen im elektronenmikroskopischen, Vol. 7. Lehre: J Cramer, pp. 614–714.

Paddock TBB (1985). Observations and comments on the diatoms *Surirella fastuosa* and *Campylodiscus fastuosus* and on other species of similar appearance. Nova Hedwigia 41: 417–444.

Parra O, González H, González M (1984). A comparison of epiphytic diatom assemblages attached to filamentous algae in lotic freshwater habitats of Chile. Gayana Bot 41: 85–117.

Patil JS, Anil AC (2000). Epibiotic community on the horseshoe crab *Tachypleus gigas*. Mar Biol 136: 699–713.

Patrick R, Reimer CW (1966). The Diatoms of United States. I. Monographs of the Academy of Natural Sciences of Philadelphia 13: 1–688.

Patrick R, Reimer CW (1975). The Diatoms of United States. II. Monographs of the Academy of Natural Sciences of Philadelphia 13: 1–213.

Pelletan J (1889). Les Diatomées. Histoire naturelle, préparation, classification et description des principales espèces. Part II. Journal de Micrographie 2: 1–364.

Pennesi C, Poulin M, De Stefano M, Romagnoli T, Totti C (2011). New insights to the ultrastructure of some marine *Mastogloia* species section Sulcatae (Bacillariophyceae), including *Mastogloia neoborneensis* sp. nov. Phycologia 50: 548–562.

Pennesi C, Poulin M, De Stefano M, Romagnoli T, Totti C (2012). Morphological studies of some marine *Mastogloia* (Bacillariophyceae) belonging to section Sulcatae, including the description of new species. J Phycol 48: 1248–1264.

Pennesi C, Poulin M, Hinz F, Romagnoli T, De Stefano M, Totti C (2013). Comparison of two new species of *Mastogloia* (Bacillariophyceae) with other small members of section Ellipticae. Phytotaxa 126: 1–21.

Peragallo H (1888). Diatomées du Midi de la France. Diatomées de la Baie de Villefranche (Alpes Maritimes). Bulletin de la Société d'Histoire Naturelle de Toulouse 22: 5–100.

Peragallo H, Peragallo M (1897–1908). Diatomées marines de France et des districts maritimes voisins. Grez-sur-Loing: Tempère.

Pero P (1893). I Laghi Alpini Valtellinesi. (Ricerche e studi sui Laghi Valtellinesi). Nuova Notarisia 4: 249–387.

Pickett-Heaps J (1989). Morphogenesis of the labiate process in the araphid pennate diatom *Diatoma vulgare*. J Phycol 25: 79–85.

Podzorski AC, Håkansson H (1987). Freshwater and marine diatoms from Palawan. Bibliotheca Diatomologica 13: 1–245.

Poulin M, Bérard-Therriault L, Cardinal A (1984a). Les diatomées benthiques de substrats durs des eaux marines et saumâtres du Québec. 1. Cocconeioideae (Achnanthales, Achnanthaceae). Le Naturaliste Canadien 111: 45–61.

Poulin M, Bérard-Therriault L, Cardinal A (1984b). Les diatomées benthiques de substrats durs des eaux marines et saumâtres du Québec. 2. Tabellarioideae et Diatomoideae (Fragilariales, Fragilariaceae). Le Naturaliste Canadien 111: 275–295.

Poulin M, Bérard-Therriault L, Cardinal A (1986). *Fragilaria* and *Synedra* (Bacillariophyceae): a morphological and ultrastructural approach. Diatom Res 1: 99–112.

Poulin M, Bérard-Therriault L, Cardinal A (1987). Les diatomées (Bacillariophyceae) benthiques de substrats durs des eaux marines et saumâtres du Québec. 7. Naviculales (Les genres *Plagiotropis* et *Entomoneis*), Epithemiales et Surilellales. Le Naturaliste Canadien 114: 67–80.

Poulin M, Bérard-Therriault L, Cardinal A, Hamilton PB (1990). Les diatomées (Bacillariophycea) benthiques de substrats durs des eaux marines et saumâtres du Québec. 9. Bacillariaceae. Le Naturaliste Canadien 117: 73–101.

Řeháková Ż (1976). Diatoms from thermal waters and mud in Piestany Spa (Slovakia). Archiv für Hydrobiologie. Supplement, Algological Studies 1149: 141–175.

Ricard M (1987). Diatomophycées. Atlas du phytoplankton marin. Vol. 2. Paris: Éditions du Centre National de la Recherche Scientifique.

Roemer SC, Hoagland KD, Rosowski JR (1984). Development of a freshwater periphyton community as influenced by diatom mucilages. Can J Botany 62: 1799–1813.

Romagnoli T, Bavestrello G, Cucchiari E, De Stefano M, Di Camillo C, Pennesi C, Puce S, Totti C (2007). Microalgal communities epibiontic on the marine hydroid *Eudendrium racemosum* in the Ligurian Sea during an annual cycle. Mar Biol 151: 537–552.

Romero O (1996a). Ultrastructure of four species of diatom genus *Cocconeis* with the description of *C. pseudocostata* spec. nov. Nova Hedwigia 63: 361–396.

Romero O (1996b). *Cocconeis sedimentaria* sp. nov. (Bacillariophyta), a marine diatom from the coastal waters of the southeastern Pacific Ocean. Diatom Res 11: 305–316.

Rosowski JR, Hoagland KD, Aloi JE (1986). Structural morphology of diatom-dominated stream biofilm communities under the impact of soil erosion. In: Evans LV, Hoagland KD, editors. Algal Biofouling. New York: Elsevier, pp. 247–299.

Ross R, Cox EJ, Karayeva NI, Mann DG, Paddock TBB, Simonsen R, Sims PA (1979). An amended terminology for the siliceous components of the diatom cell. Nova Hedwigia 64: 513–533.

Roth AW (1806). Quibus plantae novae et minus cognitae describuntur atque illustrantur. Leipzig: Catalecta Botanica.

Round FE (1971). Benthic marine diatoms. Oceanography and Marine Biology Annual Review 9: 83–139.

Round FE (1981). The Ecology of Algae. Cambridge: Cambridge University Press.

Round FE, Crawford RM, Mann DG (1990). The Diatoms. Biology & morphology of the Genera. Cambridge: Cambridge University Press.

Round FE, Sloane JF, Ebling FJ, Kitching JA (1961). The ecology of Lough Ine. X. The hydroid *Sertularia operculata* (L.) and its associated flora and fauna: ejects of transference to sheltered waters. J Ecol 49: 617–629.

Ruck E, Kociolek JP (2004). A preliminary phylogeny of the family Surirellaceae. Bibliotheca Diatomologica 50: 1–236.

Sar EA, Ferrario ME (1990). *Licmophora flabellata*. Ultrastructure and taxonomy. I. Implication. Diatom Res 5: 403–408.

Schauderna H (1983). Die Diatomeenflora aus den miozänen Seeablagerungen im Nördlinger Ries. Palaeontographica 188: 83–193.

Schmidt A, Schmidt M, Fricke H, Heiden H, Müller O, Hustedt F (1874–1959). Atlas der DiatomaceenKunde. Leipzig: Reisland.

Shim JH (1977). A taxonomic study of marine planktonic diatoms of Vancouver Island coastal warers. Proceedings of College of Natural Sciences of Seoul National University 2: 79–184.

Simonsen R (1987). Atlas and Catalogue of the Diatom Types of Friedrich Hustedt. Berlin: Cramer.

Siqueiros-Beltrones D, Guzmán del Próo S, Serviere-Zaragoza E (2005a). Main diatom taxa in the natural diet of juvenile *Haliotis fulgens* and *H. corrugata* (Mollusca: Gastropoda) in Bahía Tortugas and Bahía Asunción, B. C. S., México. Pac Sci 59: 581–592.

Siqueiros-Beltrones DA, Ibarra-Obando SE, Loya-Salinas DH (1985). An approximation to the floristic structure of the epiphytic diatoms of *Zostera marina* and its temporal variations in Bahía Falsa, San Quintín, B.C. Cienc Mar 11: 69–88.

Siqueiros-Beltrones D, López-Fuerte FO, Gárate-Lizárraga I (2005b). Structure of diatom assemblages living on prop roots of the red mangrove (*Rhizophora mangle*) from the west coast of Baja California Sur, Mexico. Pac Sci 59: 79–96.

Smith W (1853–1856). A Synopsis of the British Diatomaceae. Vol. 1. London: John Van Voorst.

Snoeijs PJM (1992). Studies in the *Tabularia fasciculata* complex. Diatom Res 7: 313–344.

Sullivan MJ (1975). Diatom communities from a Delaware salt marsh. J Phycol 11: 384–390.

Sullivan MJ (1978). Diatom community structure: taxonomic and statistical analyses of a Mississippi salt marsh. J Phycol 14: 468–475.

Sullivan MJ (1979). Epiphytic diatoms of three seagrass species in Mississippi Sound. Bulletin of Marine Science 29: 459–464.

Sullivan MJ (1980). Community structure of diatoms epiphytic on mangroves and *Thalassia* in Bimini Harbour, Bahamas. In: Ross R, editor. Proceedings of the Sixth Symposium on Recent and Fossil Diatoms. Budapest: Koeltz Science, pp. 385–398.

Sullivan MJ (1984). Community structure of epiphytic diatoms from the Gulf Coast of Florida, U.S.A. In: Proceedings of 7th Diatom Symposium of Philadelphia, pp. 373–384.

Tanaka N (1986). Adhesive strength of epiphytic diatoms on various seaweeds. B Jon Soc Sci Fish 52: 817–821.

Totti C (2003). Influence of the plume of the River Po on the distribution of subtidal microphytobenthos in the northern Adriatic Sea. Bot Mar 46: 161–178.

Totti C, Calcinai B, Cerrano C, Di Camillo C, Romagnoli T, Bavestrello G (2005). Diatom assemblages associated with *Sphaerotylus antarcticus* (Porifera, Demospongiae). J Mar Biol Assoc UK 85: 795–800.

Totti C, Cucchiari E, De Stefano M, Pennesi C, Romagnoli T, Bavestrello G (2007). Seasonal variations of epilithic diatoms on different hard substrates, in the northern Adriatic Sea. J Mar Biol Assoc Uk 87: 649–658.

Totti C, Poulin M, Romagnoli T, Perrone C, Pennesi C, De Stefano M (2009). Epiphytic diatom communities on intertidal seaweeds from Iceland. Polar Biol 32: 1681–1691.

Totti C, Romagnoli T, De Stefano M, Di Camillo CG, Bavestrello G (2011). The diversity of epizoic diatoms: relationships between diatoms and marine invertebrates. In: Seckbach J, Dubinsky Z, editors. Cellular Origin, Life in Extreme Habitats and Astrobiology. Berlin: Springer, pp. 323–343.

Tuji A (1999). A new fluorescence microscopy method to study biofilm architecture. In: Proceedings of the 14th International Diatom Symposium, pp. 321–326.

Tuji A (2000). Observation of developmental processes in loosely attached diatom (Bacillariophyceae) communities. Phycol Res 48: 75–84.

Wahrer RJ, Fryxell GA, Cox ER (1985). Studies in pennate diatoms: valve morphologies of *Licmophora* and *Campylostylus*. J Phycol 21: 206–217.

Van Der Werff A, Huls H (1957–1974). Diatomeenflora van Nederland. Den Haag: Drukkery Sprey.

Van Heurck H (1880–1885). Synopsis des Diatomées de Belgique. Atlas. Antwerp: Author's Edition.

Watanabe K (1988). Sub-ice microalgal strands in the Antarctic coastal fast ice area near Syowa Station. Jpn J Phycol 36: 221–229.

Williams DM (1985). Morphology, taxonomy and inter-relationship of the ribbed Araphid diatoms from the genera *Diatoma* and *Meridion* (Diatomaceae: Bacillariophya). Bibliotheca Diatomologica 8: 1–228.

Witkowski A, Lange-Bertalot H, Metzeltin D (2000). Diatom flora of marine coasts. Annotated Diatom Micrographs. Vol. 1. Koenigstein: Koeltz Scientific Books.

Wuchter C, Marquardt J, Krumbein WE (2003). The epizoic diatom community on four bryozoan species from Helgoland (German Bight, North Sea). Helgoland Mar Res 57: 13–19.